Improved broad-spectrum antibiotics against Gram-negative pathogens via darobactin biosynthetic pathway engineering

Sebastian Groß,[abce] Fabian Panter,[abcde] Domen Pogorevc,[abce] Carsten E. Seyfert,[abce] Selina Deckarm,[abc] Chantal D. Bader,[abc] Jennifer Herrmann,[abc] Rolf Müller*[abcd]

1

[a] Helmholtz Institute for Pharmaceutical Research Saarland (HIPS), Helmholtz Centre for Infection Research, Saarland University Campus, 66123 Saarbrücken, Germany

[b] Department of Pharmacy, Saarland University, 66123 Saarbrücken, Germany

[c] DZIF - German Centre for Infection Research, Partnersite Hannover-Braunschweig

[d] Helmholtz International Lab for Anti-Infectives, Campus E8 1, 66123 Saarbrücken, Germany

[e] These authors contributed equally

* Corresponding author

Table of contents

In silico design of the modified BGC, *darA* variants and pNOSO vector

The *Photorhabdus khanii* HGB1456 BGC sequence (GenBank accession WHZZ01000001.1) was used as template sequence to design the modified BGC. The modified BGC was organized in three transcriptional units, the first and second consisting only of the *relE* homologue and *darA*, respectively, and the third contains *darBCDE*. No recombinant promoter was placed upstream of the *relE*-like gene, whereas recombinant *T7lac*[1] and *nptII*[2,3] promoter systems (including *lacI* repressor gene and *lacO* operator in case of *T7lac* and RBSs in both cases) were placed upstream of *darA* and *darBCDE*, respectively. Two *tD1* terminator sequences were inserted upstream of the *nptII* promoter and downstream of *darBCDE*. Suppl. Table 1 lists all genetic elements including sequence origin used for the design of the modified BGC.

Suppl. Table 1. Genetic elements used in the design of the modified darobactin BGC.

Genetic element	Nucleotide position	Sequence origin (GenBank accession)	Nucleotide position in original sequence
pNOSO-relEdarABCDE			
*Sgr*DI	10,239 - 6	-	-
p15A ori	7 - 839	pACYC177 (X06402)[4]	766 - 1,598
kanR (*aph(3')-Ia*)	840 - 1,821	pACYC177 (X06402)[4]	1,816 - 2,797
*Mau*BI - ATTCTA - *Age*I	1,822 - 1,841	-	-
relE + intergenic region (including *Age*I)	1,842 - 2,153	*P. khanii* HGB1456 darobactin BGC(WHZZ01000001.1)	1,236,669 - 1,236,980
*Mre*I - ATTATC - *Xma*JI	2,154 - 2,173	-	-
T7lac promoter (including *lacI* and *lacO*)	2,174 - 3,734	pET-10[1]	3498 - 5732
darA + intergenic region	3,735 - 4,307	*P. khanii* HGB1456 darobactin BGC(WHZZ01000001.1)	1,236,987 - 1,237,559
*Pst*I – TCCTGA - *Bam*HI	4,308 - 4,325	-	-
tD1 terminator	4,326 - 4,386	*Myxococcus xanthus* phage Mx8[5]	-
*Not*I	4,387 - 4,394	-	-
nptII promoter	4,395 - 4,548	pUC18-Zeo-mx8-nptII-corO[2] / neomycin phosphotransferase II resistance gene from Tn5[3]	-
darBCDE	4,549 - 10,169	*P. khanii* HGB1456 darobactin BGC(WHZZ01000001.1)	1,237,560 - 1,243,180
*Spe*I - TCCTGA - *Pac*I	10,170 - 10,189	-	-
tD1 terminator	10,190 - 10,238	*M. xanthus* phage Mx8[5]	-
darFG			
*Spe*I	1 - 6	-	-
darF	7 - 1,083	*P. luteoviolacea* S4054 (NZ_CP015412)	976,996 - 975,920 (reverse DNA strand)
darG	1,084 - 2,847	*P. luteoviolacea* S4054 (NZ_CP015412)	970,404 - 968,641 (reverse DNA strand
*Pac*I	2,848 - 2,855	-	-

Additional to natively present unique restriction endonuclease recognition sites (R-sites), numerous R-sites were introduced into the modified BGC to allow genetic manipulation using restriction hydrolysis/DNA ligation cloning techniques. Furthermore, two *Nde*I R-sites were removed from the

BGC by synonymous codon substitutions, since *Nde*I was required as unique R-site downstream of the *T7lac* promoter for *darA* exchange or exchange of the *T7lac* promoter itself. Suppl. Table 2 summarizes unique R-sites and their function.

Suppl. Table 2. Function of important R-sites in the modified darobactin BGC. [a] R-site upstream of MauBI R-site in pUC57-relEdarABCDE (not present in pNOSO-relEdarABCDE), [b] R-site present two times in the modified darobactin BGC, [c] R-sites was not used for cloning experiments in this work, [d] R-site downstream of SgrDI R-site in pUC57-relEdarABCDE (not present in pNOSO-relEdarABCDE).

R-site	**Function**
*Kpn*I[a]	pSynbio1 subcloning
*Mau*BI	pNOSO subcloning
*Age*I[b]	Removal of *relE* homologue
*Mre*I[c]	Exchange of *T7lac* promoter
*Xma*JI	Exchange of *T7lac* promoter
*Nde*I	Exchange of *T7lac* promoter or *darA*
*Pst*I[c]	Exchange of *darA*
*Bam*HI	Exchange of *darA*
*Not*I	Exchange of *nptII* promoter
*Xho*I	Exchange of *nptII* promoter
*Spe*I	Introduction of *darFG*
*Pac*I	Introduction of *darFG*
*Sgr*DI	pNOSO subcloning
*Pme*I[d]	pSynbio1 subcloning

The *darA* sequence plus 396 bp downstream intergenic region was used as template for the design of *darA* variants with altered core sequences. The three nucleotides CAT were placed upstream of *darA*, thus generating a *Nde*I R-site together with the adjacent ATG start codon. *Nco*I, *Pst*I and *Bam*HI R-sites (with short random spacers in between) were placed downstream of the intergenic region. The mutations that were introduced into the core sequence of *darA* are listed in Table 1 of the manuscript.

The pNOSO vector contains the *p15A* origin of replication (ori) and the *aph(3')-Ia* gene encoding aminoglycoside-3'-phosphotransferase-Ia (mediating kanamycin resistance) for maintenance in *E. coli* and selection, respectively. Two unique R-sites, *Sal*I and *Sgr*DI (with short random spacer in between), were placed upstream of the *p15A* ori. Furthermore, a unique *Mau*BI R-site was placed downstream of the *aph(3')-Ia* terminator. The genetic elements of pNOSO are listed in Suppl. Table 1.

The *darFG* fragment was designed based on the template sequence from *Pseudoalteromonas luteoviolacea* S4054 (GenBank accession NZ_CP015412) (Suppl. Figure 1). We placed a *Spe*I R-site upstream of *darF* and a *Pac*I R-site downstream of *darG*, allowing cloning of *darFG* into pNOSO-darABCDE. Genetic elements of *darFG* are listed in Suppl. Table 1.

Suppl. Figure 1. Schematic overview of the darobactin BGC from P. luteoviolacea *S4054 including* darF *and* darG (purple arrows), darA *(green arrow),* darBCD *(light grey arrows) and* darE *(blue arrow).*

All sequences were deposited in GenBank database under the accession numbers provided in Supplementary Data.

Cloning of expression constructs

All DNA sequences designed *in silico* were chemically synthesized by GenScript Biotech Corporation (Piscataway, New Jersey (US)). Sequence-verified DNA synthesis fragments were delivered in pUC57 standard vectors harbouring an *ampR* (*bla*) gene for selection on ampicillin. Restriction endonuclease hydrolysis and DNA ligation were performed according to the manufacturer`s information protocols. Handling of DNA and PCRs were performed according to standard protocols.[6] *E. coli* transformation was carried out via electroporation in cuvettes with 1 mm electrode distance using 1,350 Vcm^{-1}, 10 µF and 600 Ω as conditions. The transformed cells were resuspended in 1 mL LB medium (composition described below) and incubated for 90 min before selection on LB agar medium overnight. Selected clones were cultivated in 5 mL of liquid LB medium for 16 h and plasmid DNA was subsequently isolated from 2 mL culture using alkaline lysis. The correctness of the isolated constructs was verified by restriction hydrolysis.

pSynbio1-relEdarABCDE was generated by ligation of the modified BGC into pSynbio1 after restriction hydrolysis of pSynbio1 and pUC57-relEdarABCDE with *Kpn*I and *Pme*I. pNOSO-relEdarABCDE was generated by ligation of the modified BGC into pNOSO after restriction hydrolysis of pNOSO and pUC57-relEdarABCDE with *Mau*BI and *Sgr*DI. pNOSO-darABCDE was generated after removal of the *relE*-like gene by restriction hydrolysis with *Age*I and subsequent vector re-ligation. pNOSO-darABCDEFG was generated by ligation of *darFG* into pNOSO-darABCDE after restriction hydrolysis of pNOSO-darABCDE and pUC57-darFG with *Spe*I and *Pac*I. pNOSO-darABCDE-B to –E, and pNOSO-darABCDE-1 to -21 were generated by restriction hydrolysis of pNOSO-darABCDE with *Nde*I and *Bam*HI to remove *darA* and introduction of the respective *darA*-variants by ligation. Suppl. Table 3 summarizes all restriction hydrolysis/DNA ligation cloning steps performed in this study.

For heterologous expression, purification and *in vitro* characterisation of DarF (see subsection below), the *darF* gene was amplified from pUC57-darFG via PCR using the primers darF-fw (ATACCCATGGG GCATACACTTACCAATGAACTAC) and darF-rv (ATACCCTCGAGTTATTTTAAGCGCTCTAATGTTTCT), which contain additional sequence overhangs with *Nco*I and *Xho*I R-sites, respectively. The pHisSUMOTEV-

darF expression construct was generated by ligation of *darF* into pHisSUMOTEV[7] after restriction hydrolysis with *Nco*I and *Xho*I.

All strains and plasmids generated in this work are listed in the Supplementary Data file.

Suppl. Table 3. Summary of restriction hydrolysis/DNA ligation cloning steps. GSP: gene synthesis product.

Cloning product	**Vector**	**Insert**	**Insert source**	**Restriction endonuclease**
pSynbio1-relEdarABCDE	pSynbio1	relEdarABCDE	pUC57-relEdarABCDE (GSP)	*Kpn*I/*Pme*I
pNOSO-relEdarABCDE	pNOSO	relEdarABCDE	pUC57-relEdarABCDE (GSP)	*Mau*BI/*Sgr*DI
pNOSO-darABCDE	pNOSO-relEdarABCDE	-	-	*Age*I
pNOSO-darABCDE-nptII-syncor	pNOSO-darABCDE	nptII-syncor	PCR	*Xma*JI/*Nde*I
pNOSO-darABCDE-nptII-synarg	pNOSO-darABCDE	nptII-synarg	PCR	*Xma*JI/*Nde*I
pNOSO-darABCDE-nptII-T7	pNOSO-darABCDE	nptII-T7	PCR	*Xma*JI/*Nde*I
pNOSO-darABCDE-Pm-synarg	pNOSO-darABCDE	Pm-synarg	PCR	*Xma*JI/*Nde*I
pNOSO-darABCDE-Pm-T7	pNOSO-darABCDE	Pm-T7	PCR	*Xma*JI/*Nde*I
pNOSO-darABCDE-tet-synarg	pNOSO-darABCDE	tet-synarg	PCR	*Xma*JI/*Nde*I
pNOSO-darACDE	pNOSO-darACDE-cmR	-	-	*Bsa*I
pNOSO-darABDE	pNOSO-darABDE-cmR	-	-	*Bsa*I
pNOSO-darABCE	pNOSO-darABCE-cmR	-	-	*Bsa*I
pNOSO-darABCD	pNOSO-darABCD-cmR	-	-	*Bsa*I
pNOSO-darABCDEF	pNOSO-darABCDEF-cmR	-	-	*Bsa*I
pNOSO-darABCDEG	pNOSO-darABCDEG-cmR	-	-	*Bsa*I
pNOSO-darABCDEFG	pNOSO-darABCDE	*darFG*	pUC57-darFG (GSP)	*Spe*I/*Pac*I
pNOSO-darABCDE-B	pNOSO-darABCDE	*darA*-B	pUC57-darA-B (GSP)	*Nde*I/*Bam*HI
pNOSO-darABCDE-C	pNOSO-darABCDE	*darA*-C	pUC57-darA-C (GSP)	*Nde*I/*Bam*HI
pNOSO-darABCDE-D	pNOSO-darABCDE	*darA*-D	pUC57-darA-D (GSP)	*Nde*I/*Bam*HI
pNOSO-darABCDE-E	pNOSO-darABCDE	*darA*-E	pUC57-darA-E (GSP)	*Nde*I/*Bam*HI
pNOSO-darABCDE-1	pNOSO-darABCDE	*darA*-1	pUC57-darA-1 (GSP)	*Nde*I/*Bam*HI
pNOSO-darABCDE-2	pNOSO-darABCDE	*darA*-2	pUC57-darA-2 (GSP)	*Nde*I/*Bam*HI
pNOSO-darABCDE-4	pNOSO-darABCDE	*darA*-4	pUC57-darA-4 (GSP)	*Nde*I/*Bam*HI
pNOSO-darABCDE-5	pNOSO-darABCDE	*darA*-5	pUC57-darA-5 (GSP)	*Nde*I/*Bam*HI
pNOSO-darABCDE-6	pNOSO-darABCDE	*darA*-6	pUC57-darA-6 (GSP)	*Nde*I/*Bam*HI
pNOSO-darABCDE-7	pNOSO-darABCDE	*darA*-7	pUC57-darA-7 (GSP)	*Nde*I/*Bam*HI
pNOSO-darABCDE-8	pNOSO-darABCDE	*darA*-8	pUC57-darA-8 (GSP)	*Nde*I/*Bam*HI
pNOSO-darABCDE-9	pNOSO-darABCDE	*darA*-9	pUC57-darA-9 (GSP)	*Nde*I/*Bam*HI
pNOSO-darABCDE-10	pNOSO-darABCDE	*darA*-10	pUC57-darA-10 (GSP)	*Nde*I/*Bam*HI
pNOSO-darABCDE-11	pNOSO-darABCDE	*darA*-11	pUC57-darA-11 (GSP)	*Nde*I/*Bam*HI
pNOSO-darABCDE-12	pNOSO-darABCDE	*darA*-12	pUC57-darA-12 (GSP)	*Nde*I/*Bam*HI
pNOSO-darABCDE-13	pNOSO-darABCDE	*darA*-13	pUC57-darA-13 (GSP)	*Nde*I/*Bam*HI
pNOSO-darABCDE-14	pNOSO-darABCDE	*darA*-14	pUC57-darA-14 (GSP)	*Nde*I/*Bam*HI
pNOSO-darABCDE-15	pNOSO-darABCDE	*darA*-15	pUC57-darA-15 (GSP)	*Nde*I/*Bam*HI
pNOSO-darABCDE-16	pNOSO-darABCDE	*darA*-16	pUC57-darA-16 (GSP)	*Nde*I/*Bam*HI
pNOSO-darABCDE-17	pNOSO-darABCDE	*darA*-17	pUC57-darA-17 (GSP)	*Nde*I/*Bam*HI
pNOSO-darABCDE-18	pNOSO-darABCDE	*darA*-18	pUC57-darA-18 (GSP)	*Nde*I/*Bam*HI
pNOSO-darABCDE-19	pNOSO-darABCDE	*darA*-19	pUC57-darA-19 (GSP)	*Nde*I/*Bam*HI
pNOSO-darABCDE-20	pNOSO-darABCDE	*darA*-20	pUC57-darA-20 (GSP)	*Nde*I/*Bam*HI
pNOSO-darABCDE-21	pNOSO-darABCDE	*darA*-21	pUC57-darA-21 (GSP)	*Nde*I/*Bam*HI

Targeted gene deletions

Independent seamless deletions of *darB*, *darC*, *darD* and *darE* from pNOSO-darABCDE (to obtain pNOSO-darACDE, pNOSO-darABDE, pNOSO-darABCE and pNOSO-darABCD) and deletions of *darF* and *darG* from pNOSO-darABCDEFG (to obtain expression constructs with *darABCDEF* or *darABCDEG*) were carried out using Red/ET recombineering[8] in combination with restriction hydrolysis and vector re-ligation (Suppl. Figure 2).

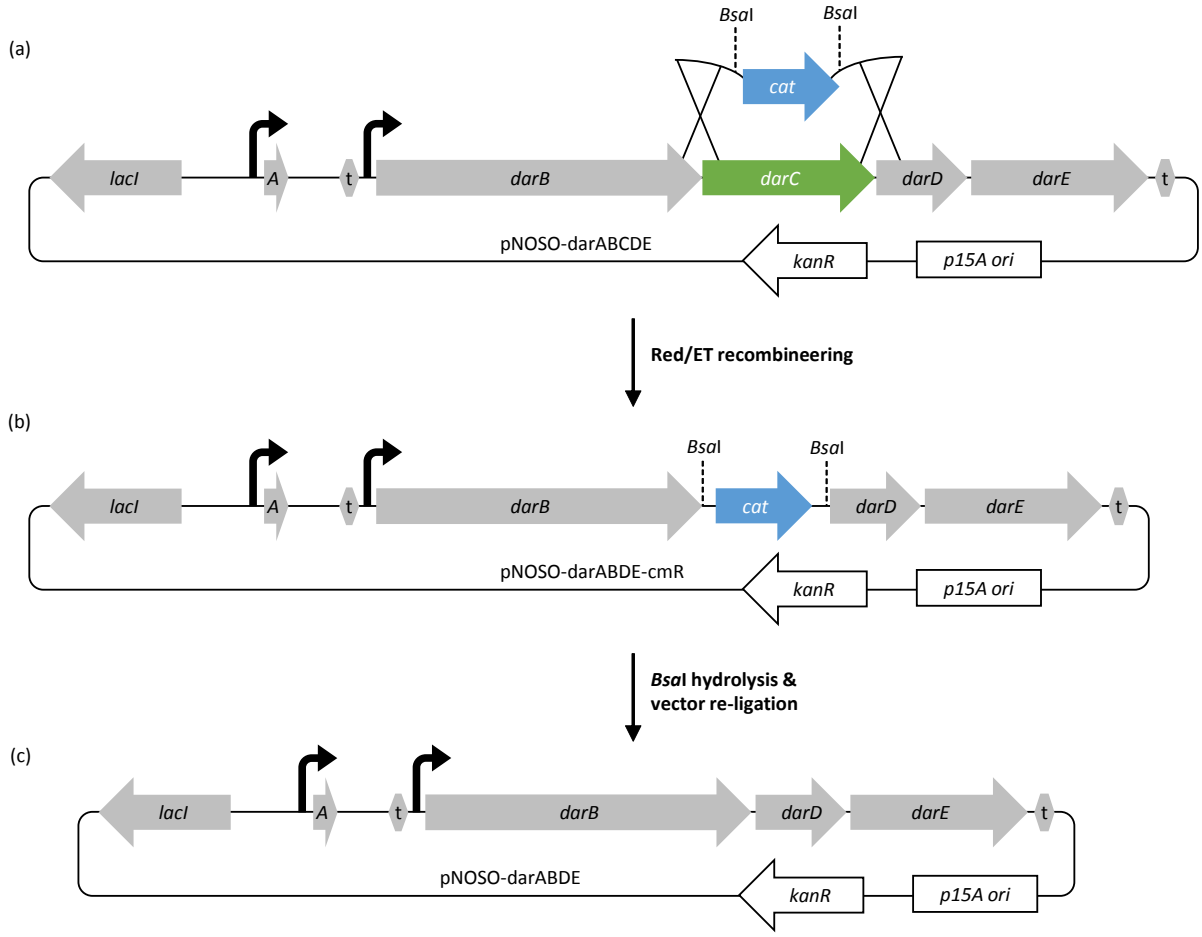

Suppl. Figure 2. Seamless gene deletion on the example of darC*. (a) Replacement of* darC *(shown in green) in pNOSO-darABCDE by chloramphenicol resistance-mediating* cat *gene PCR product (shown in blue) via Red/ET recombineering. (b) Removal of* cat *via restriction hydrolysis using* BsaI*. (c) Re-ligation of the vector yields pNOSO-darABDE.*

First, the *cat* gene encoding chloramphenicol *O*-acetyltransferase (mediating chloramphenicol resistance) was amplified by PCR using pMYC20[9] as template. Apart from pMYC20 binding sites, primers contained tail sequences with *Bsa*I R-sites and 50 bp sequences that are homologous to the deleted gene. *Bsa*I is a type IIS restriction endonuclease cutting outside of its recognition sequence, thereby allowing the generation of variable and unique 5 bp sticky ends for ligation. All oligonucleotide primers used for the gene deletion experiments and a summary of all PCRs performed are listed in Suppl. Table 4 and Suppl. Table 5, respectively.

Suppl. Table 4. Oligonucleotides used in seamless gene deletion experiments.

Oligonucleotide	Sequence (5'-3')
Cm-DarB-F	GCGCAGGGGATCAAGATCTGATCAAGAGACAGGATAAGGAGGTACAGATTGGAGACCTACCTGTGACGGAAGATCACTTCG
Cm-DarB-R	CTCTCTGTTATGTATGCCTTTTTTTCTGATTTCTATATCCATAATTAATCAATCCGAGACCGCACACGGTCACACTGCTTC
Cm-DarC-F	CTACCTATTTGGTGAATTATAGAAAATTATCCGCCACTAAATTTTTGTGAGGAGACCTACCTGTGACGGAAGATCACTTCG
Cm-DarC-R	TTTATATGATTTACAGATATTCATCATGCTAATCATTTTATTCAATCCTTTCACCGAGACCGCACACGGTCACACTGCTTC
Cm-DarD-F	GCTTTGGTAAGAATAAATTAGTTAATAATGATACAGTAAGGATTGAATAAGGAGACCTACCTGTGACGGAAGATCACTTCG
Cm-DarD-R	TATGGGGATTATTGTGTCCATAAAGAACTCCTTTATTATGTTATTTATGCTTATCGAGACCGCACACGGTCACACTGCTTC
Cm-DarE-F	CGTTTTCTGACAGAATATTAACGATGAGGGATGGCCACTTGCTTGTTTGAGGAGACCTACCTGTGACGGAAGATCACTTCG
Cm-DarE-R	CGGTTCCGGGCCCTTGCAGGGTGGTTAATTAATCAGGAACTAGTTAGAATTCAACGAGACCGCACACGGTCACACTGCTTC
Cm-DarF-F	GTGGAACCGGCGGTTTGTTGGAGACAATAAAACAAACCATCGCGGCGTAAGGAGACCTACCTGTGACGGAAGATCACTTCG
Cm-DarF-R	TGATAAACGATGCCTTGTGCACTGATCTGCATGTTTTAAATCGACTCTTCTTACCGAGACCGCACACGGTCACACTGCTTC
Cm-DarG-F	ATGACATCATAAACACAAAACTCATAGAAACATTAGAGCGCTTAAAATAAGGAGACCTACCTGTGACGGAAGATCACTTCG
Cm-DarG-R	CCCGGAACCTTGCGGTTCCGGGCCCTTGCAGGGTGGTTAATTAATAGAATTTATCGAGACCGCACACGGTCACACTGCTTC

Suppl. Table 5. Summary of PCRs performed in seamless gene deletion experiments.

PCR product	Template DNA	Forward primer	Reverse primer
cmR (*darB*)	pMYC20	Cm-DarB-F	Cm-DarB-R
cmR (*darC*)	pMYC20	Cm-DarC-F	Cm-DarC-R
cmR (*darD*)	pMYC20	Cm-DarD-F	Cm-DarD-R
cmR (*darE*)	pMYC20	Cm-DarE-F	Cm-DarE-R
cmR (*darF*)	pMYC20	Cm-DarF-F	Cm-DarF-R
cmR (*darG*)	pMYC20	Cm-DarG-F	Cm-DarG-R

For Red/ET recombineering, 1.4 mL LB medium was inoculated with *E. coli* GB05-red and grown at 37 °C to OD_{600} 0.2. After addition of 40 µL 10 % (w/v) L-arabinose, the cultivation was continued until OD_{600} 0.4 was reached. The cells were harvested, washed twice in ice-cold ddH_2O and finally re-suspended in 30 µL of ddH_2O. The *cat* PCR product was transformed into *E. coli* GB05-red pNOSO-darABCDE or *E. coli* GB05-red pNOSO-darABCDEFG via electroporation as described above. Plasmid DNA from the fully overgrown LB agar selection plate (kanamycin and chloramphenicol) was isolated using alkaline lysis, followed by another transformation step of 100 ng of the isolated plasmid mixture into *E. coli* NEB10β. Again, we selected clones harbouring the correct recombination products on kanamycin and chloramphenicol. After the plasmid isolation, we verified the clones by restriction analysis. Next, the recombination product was hydrolysed with *Bsa*I and re-ligated to remove *cat* from the construct, leading to a clean deletion without leftover R-sites. Clones which lost their resistance towards chloramphenicol were selected for plasmid isolation and restriction analysis. Suppl. Table 6 lists all gene deletion plasmids that were generated in this work.

Suppl. Table 6. Constructs generated after Red/ET recombineering and removal of cat (cmR) by restriction hydrolysis with BsaI.

Product generated	Description	Vector used for Red/ET	Red/ET product
pNOSO-darACDE	Deletion of *darB*	pNOSO-darABCDE	pNOSO-darACDE-cmR
pNOSO-darABDE	Deletion of *darC*	pNOSO-darABCDE	pNOSO-darABDE-cmR
pNOSO-darABCE	Deletion of *darD*	pNOSO-darABCDE	pNOSO-darABCE-cmR
pNOSO-darABCD	Deletion of *darE*	pNOSO-darABCDE	pNOSO-darABCD-cmR
pNOSO-darABCDEG	Deletion of *darF*	pNOSO-darABCDEFG	pNOSO-darABCDEG-cmR
pNOSO-darABCDEF	Deletion of *darG*	pNOSO-darABCDEFG	pNOSO-darABCDEF-cmR

Cultivation of strains to screen for production of darobactins

E. coli HS996, NEB10β and GB05-red strains were used for cloning and manipulation of the modified BGC. Cultivation of cloning strains was exclusively performed in LB medium (10 g/L tryptone, 5 g/L NaCl, 5 g/L yeast extract, pH 7.6) at 30 °C. *E. coli* BL21 (DE3) was used as heterologous expression host. All small scale fermentations to screen for the production of darobactins were performed in 50 mL scale in unbaffled 300 mL shaking flasks at 30 °C for 3 days and 180 rpm on an orbital shaker (Orbitron/Multitron, Infors HT) using FM cultivation medium (12.54 g/L K_2HPO_4, 2.31 g/L KH_2PO_4, 5 g/L NaCl, 12 g/L yeast extract, 4 g/L D(+) glucose, 1 g/L NH_4Cl, 0.24 g/L $MgSO_4$, pH 7.6) supplemented with 1 mg/L vitamin B_{12} after sterilization. Production screening cultures were inoculated with 5 mL of a 25 mL LB seed culture that grew for 16 h at 30 °C and 180 rpm. Ampicillin (100 µg/mL; pUC57- and pSynbio1-based expression constructs), chloramphenicol (34 µg/mL; Red/ET deletion constructs prior *cat* removal) and kanamycin (50 µg/mL; pNOSO-based expression constructs) were used as selection markers.

The initial evaluation of different media, *E. coli* strains and expression constructs is described in the respective section below. Cultivation of strains for purification of darobactins A and 9 and DarF, as well as cultivation of strains used for determination of the MICs are described in the respective sections below.

UHPLC-HRMS analysis of production screening cultures

The fermentation broth of 50 mL screening cultures was centrifuged at 7,750 × g for 15 min at 4 °C. The supernatant was directly analysed using uHPLC-HRMS. An UltiMate 3000 LC System (Dionex, Sunnyvale, California (US)) with a Acquity UPLC BEH C-18 column (1.7 µm, 100 x 2 mm; Waters Corporation, Milford, Massachusetts (US)), equipped with a VanGuard BEH C-18 (1.7 µm; Waters Corp.) guard column, was coupled to an Apollo II ESI source (Bruker Daltonics; Billerica, Massachusetts

(US)) and hyphenated to maXis 4G ToF mass spectrometer (Bruker Daltonics). Separation was performed at a flow rate of 0.6 mL/min (eluent A: deionised H_2O + 0.1 % formic acid (FA), eluent B: acetonitrile + 0.1 % FA) at 45 °C using the following gradient: 5 % B for 30 s, followed by a linear gradient up to 95 % B in 18 min and a constant percentage of 95 % B for further 2 min. Original conditions were adjusted with 5 % B within 30 s and kept constant for 1.5 min. The LC flow was split to 75 µL/min before entering the mass spectrometer. Mass spectra were acquired in centroid mode ranging from 150–2,500 m/z at a 2 Hz full scan rate. Mass spectrometry source parameters were set to 500 V as end plate offset, 4000 V as capillary voltage, 1 bar nebulizer gas pressure, 5 L/min dry gas flow and 200 °C dry temperature. For MS^2 experiments, CID (collision-induced dissociation) energy was ramped from 35 eV for 500 m/z to 45 eV for 1,000 m/z. MS full scan acquisition rate was set to 2 Hz and MS^2 spectra acquisition rates were ramped from 1 to 4 Hz for precursor ion intensities of 10 kcts to 1,000 kcts.

Initial evaluation of different heterologous expression constructs, strains and cultivation conditions

Initially we evaluated different *E. coli* expression strains, cultivation media and expression constructs to reach a darobactin A production titre sufficient for compound purification. All cultivations were performed in 50 mL scale in unbaffled 300 mL shaking flasks at 30 °C for 3 days and 180 rpm on an orbital shaker as described in the Cultivation of strains section. *E. coli* BL21 (DE3), *E. coli* Lemo21 (DE3) and *E. coli* Rosetta2 (DE3) were evaluated as expression strains. LB medium (described above), 2TY medium (16 g/L tryptone, 5 g/L NaCl, 10 g/L yeast extract, pH 7.0), SB medium (32 g/L peptone, 5 g/L NaCl, 20 g/L yeast extract, pH 7.0), M medium (10 g/L tryptone, 10 g/L NaCl, 5 g/L yeast extract, 10 g/L KH_2PO_4, pH 6.5), TB medium (10 g/L tryptone, 4 g/L glycerol, 20 g/L yeast extract, 10 g/L, 50 mM KH_2PO_4 (pH 8.0), pH 7.2), TSB medium (17 g/L peptone from casein, 3 g/L peptone from soymeal, 2.5 g/L D(+) glucose, 5 g/L NaCl, 2.5 g/L K_2HPO_4, pH 7.3), SB2-2Y medium (SB medium with 40 g/L yeast extract), FM medium (described above) and FM-2Y medium (FM medium with 24 g/L yeast extract) were evaluated as cultivation media. Each medium was supplemented with 1 mg/L vitamin B_{12} after sterilization and the gene expression of *darA* and the T7 RNA polymerase was induced by addition of 0.1 mM isopropyl ß-D-1-thiogalactopyranoside (IPTG) after an OD_{600} 0.7 was reached. Furthermore, we compared the darobactin A production upon expression of the high-copy plasmids pUC57-relEdarABCDE and pSynbio1-relEdarABCDE, as well as the low-copy plasmid pNOSO-relEdarABCDE in *E. coli* BL21 (DE3). Since we observed more impurities in the base peak chromatograms (BPC) after expression of the high-copy plasmids (Suppl. Figure 3) and the highest relative darobactin A production

(based on the mass peak intensity) in *E. coli* BL21 (DE3) pNOSO-relEdarABCDE, we used this strain cultivated in FM medium as basis for all following experiments.

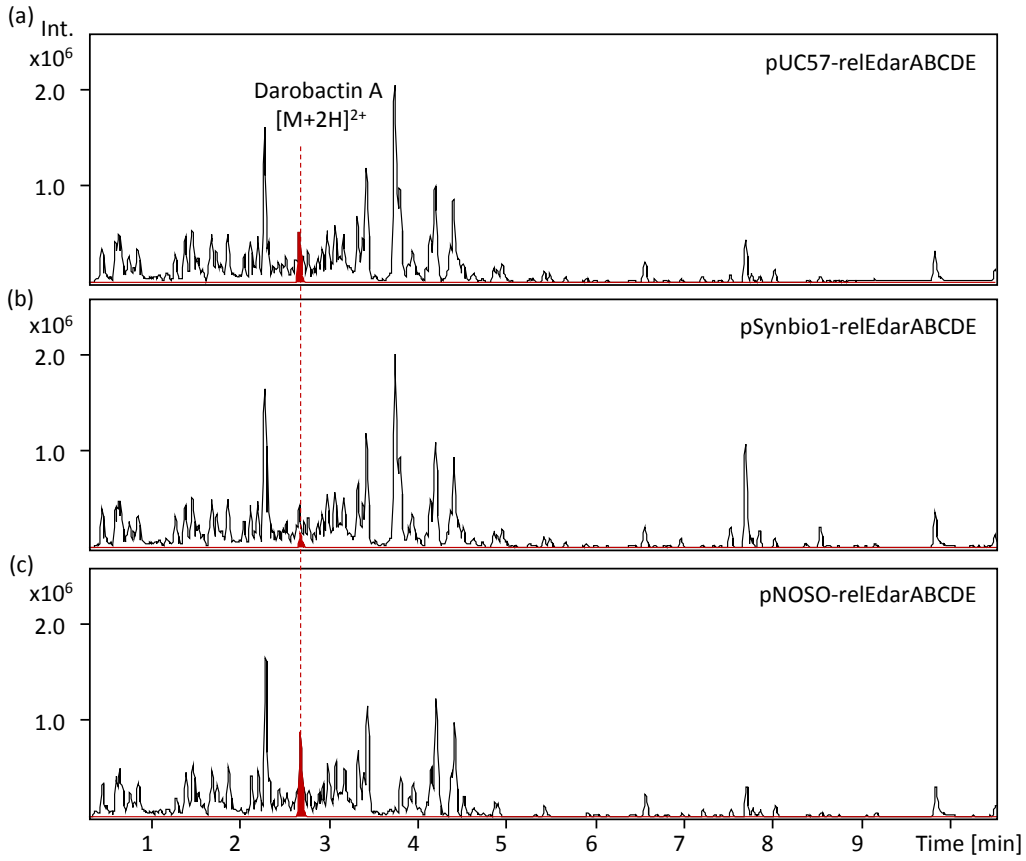

Suppl. Figure 3. Chromatogram of the E. coli *BL21 (DE3) pUC57-relEdarABCDE (a),* E. coli *BL21 (DE3) pSynbio1-relEdarABCDE (b) and* E. coli *BL21 (DE3) pNOSO-relEdarABCDE culture supernatant. The red trace displays the darobactin A EIC for the* $[M+2H]^{2+}$ *species at m/z 483.710 ±0.02 Da. The black trace displays the BPC of the fermentation supernatant.*

Induction and repression of T7 RNA polymerase expression and *T7lac* promoter-regulated *darA* gene expression

Since we observed higher darobactin A production (based on peak intensity in the MS) after not inducing the *darA* and T7 RNA polymerase gene expression compared to induction with 0.1 mM IPTG (data not shown), we tested how different inducer concentrations (10 nM, 1 nM, 0.1 nM IPTG) or repressor concentrations (0.5 %, 1.5 %, 5 % D(+) glucose) during cultivation of *E. coli* BL21 (DE3) pNOSO-darABCDE in FM medium affect the production level of darobactin A. uHPLC-HRMS analysis of the culture supernatant and determination of the darobactin A peak surface area (described in section Determination of the MS peak area under curve (AUC) ratio) revealed that the tested IPTG concentrations had no significant impact on the darobactin A production level (Suppl. Table 7). The

supplementation of 1.5 % and 5 % D(+) glucose) resulted in a ten-fold reduction of the darobactin A production titre.

Suppl. Table 7. Influence of different IPTG and D(+) glucose concentrations on the darobactin A production level after cultivation of E. coli *BL21 (DE3) pNOSO-darABCDE in FM medium. In the control no IPTG and D(+) glucose were supplemented during cultivation. AUC: area under curve.*

IPTG/ D(+) glucose conc.	**AUC relative to control [%]**
Control	100
10 nM IPTG	101
1 nM IPTG	92
0.1 nM IPTG	95
0.5 % D(+) glucose	106
1.5 % D(+) glucose	11
5 % D(+) glucose	10

UHPLC-HRMS chromatograms displaying all observed darobactin derivatives

This section displays extracted ion chromatogram (EIC) traces displaying the most abundant $[M+2H]^{2+}$ ion for all observed darobactin derivatives. The EIC traces are depicted in red, the corresponding BPCs are depicted in black. All UuHPLC-HRMS EIC chromatograms were also traced in the *E. coli* BL21 (DE3) blank extract to double check for the absence of the corresponding peak in the blank. In case of darobactins 6, 8 and 18, the masses of the respective expected darobactins (without the adducts) shown in the chromatograms and main text Table 1 have not been detected.

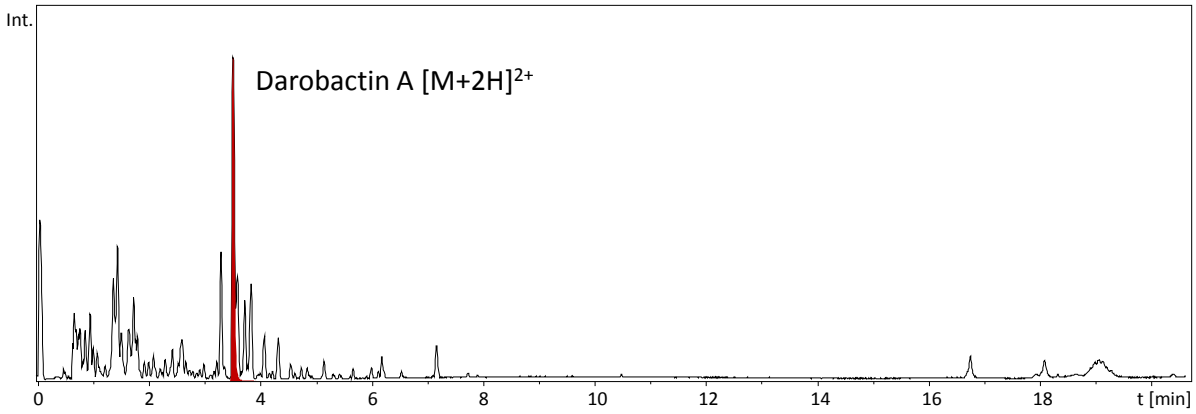

Suppl. Figure 4. Chromatogram of the E. coli *BL21 (DE3) pNOSO-darABCDE culture supernatant. The red trace displays the darobactin A EIC for the $[M+2H]^{2+}$ species at m/z 483.710 ±0.02 Da. The black trace displays the BPC of the fermentation supernatant.*

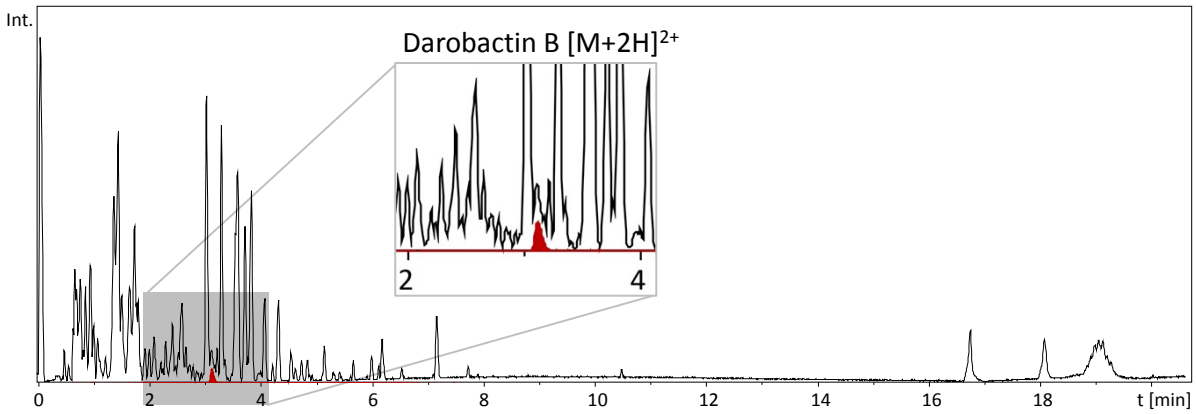

Suppl. Figure 5. Chromatogram of the E. coli *BL21 (DE3) pNOSO-darABCDE-B culture supernatant. The red trace displays the darobactin B EIC for the $[M+2H]^{2+}$ species at m/z 525.251 ±0.02 Da. The black trace displays the BPC of the fermentation supernatant. The grey area highlights the magnification area.*

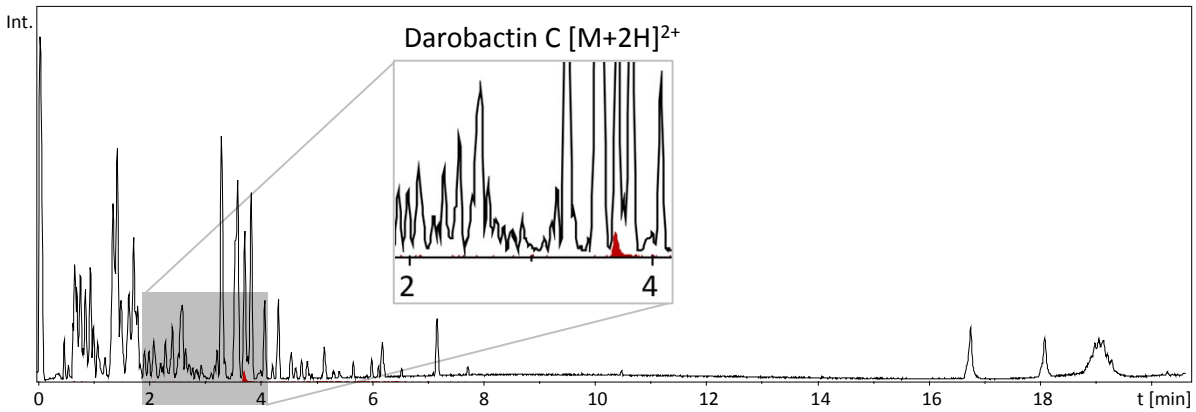

Suppl. Figure 6. Chromatogram of the E. coli *BL21 (DE3) pNOSO-darABCDE-C culture supernatant. The red trace displays the darobactin C EIC for the $[M+2H]^{2+}$ species at m/z 484.207 ±0.02 Da. The black trace displays the BPC of the fermentation supernatant. The grey area highlights the magnification area.*

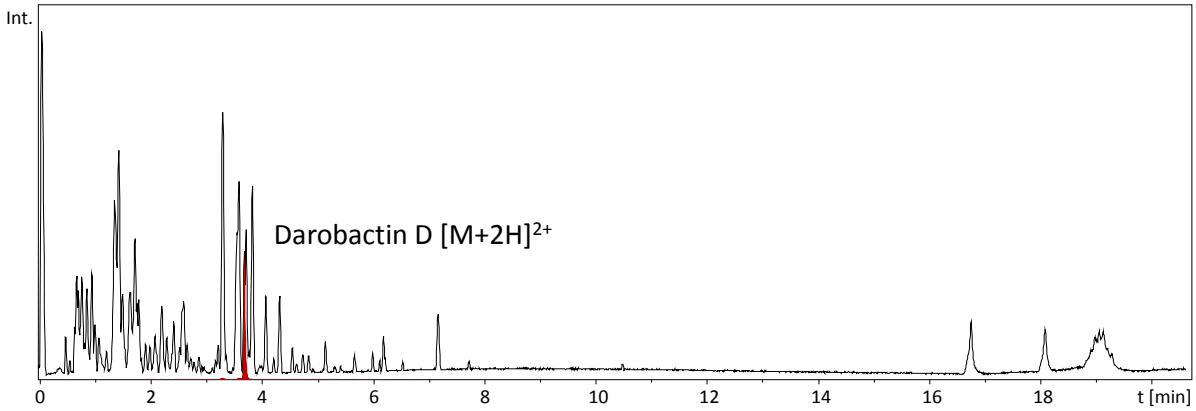

Suppl. Figure 7. Chromatogram of the E. coli *BL21 (DE3) pNOSO-darABCDE-D culture supernatant. The red trace displays the darobactin D EIC for the $[M+2H]^{2+}$ species at m/z 491.712 ±0.02 Da. The black trace displays the BPC of the fermentation supernatant.*

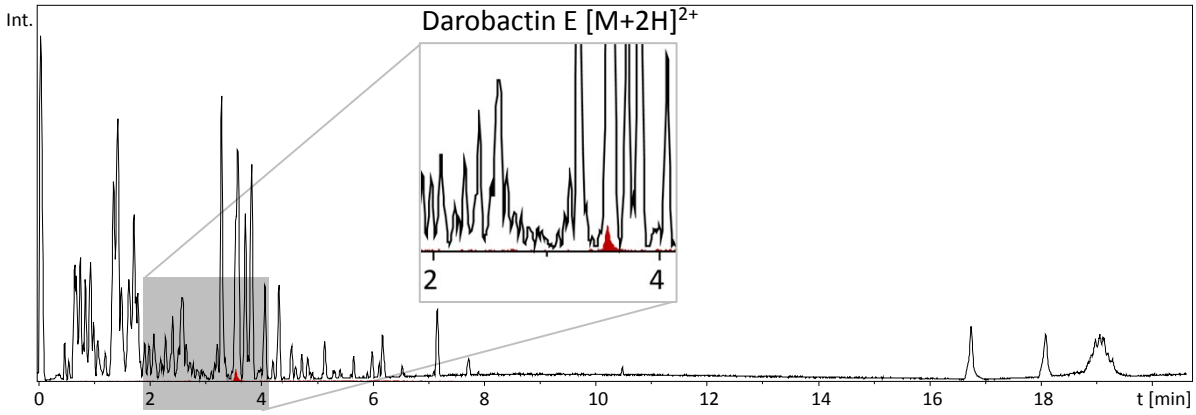

Suppl. Figure 8. Chromatogram of the E. coli *BL21 (DE3) pNOSO-darABCDE-E culture supernatant. The red trace displays the darobactin E EIC for the [M+2H]$^{2+}$ species at m/z 470.204 ±0.02 Da. The black trace displays the BPC of the fermentation supernatant. The grey area highlights the magnification area.*

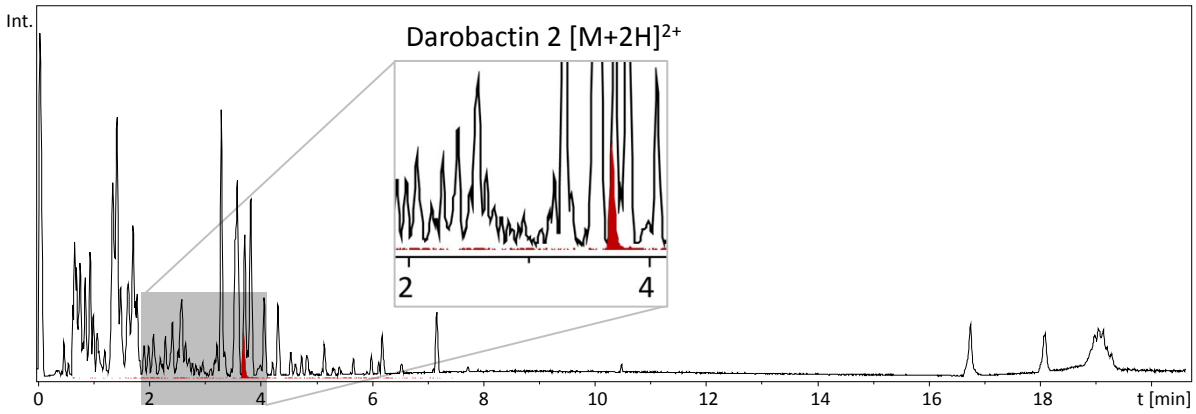

Suppl. Figure 9. Chromatogram of the E. coli *BL21 (DE3) pNOSO-darABCDE-2 culture supernatant. The red trace displays the darobactin 2 EIC for the [M+2H]$^{2+}$ species at m/z 491.215 ±0.02 Da. The black trace displays the BPC of the fermentation supernatant. The grey area highlights the magnification area.*

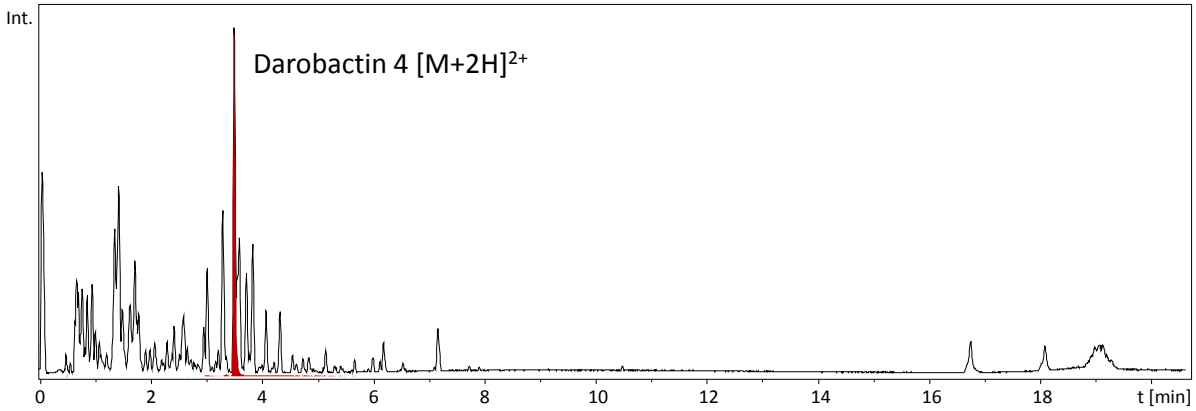

Suppl. Figure 10. Chromatogram of the E. coli *BL21 (DE3) pNOSO-darABCDE-4 culture supernatant. The red trace displays the darobactin 4 EIC for the [M+2H]$^{2+}$ species at m/z 490.717 ±0.02 Da. The black trace displays the BPC of the fermentation supernatant.*

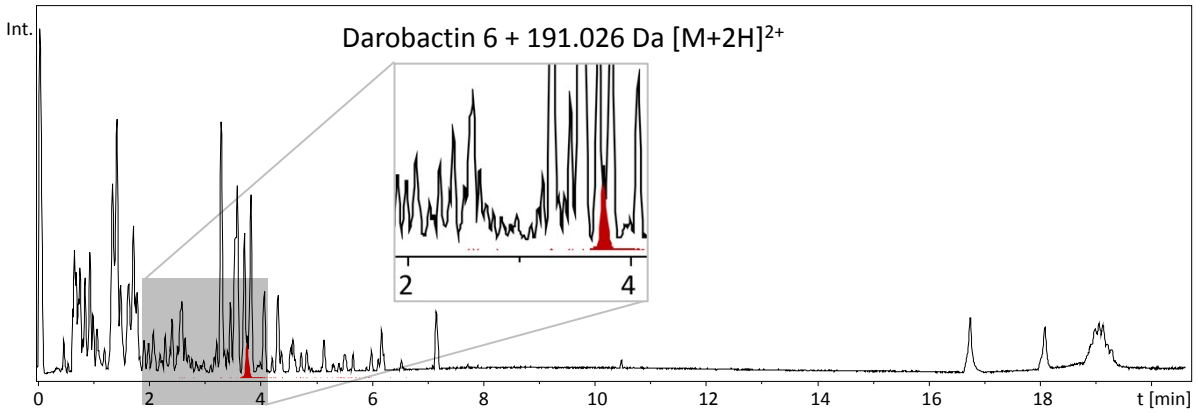

Suppl. Figure 11. Chromatogram of the E. coli *BL21 (DE3) pNOSO-darABCDE-6 culture supernatant. The red trace displays the darobactin 6 + 191.026 EIC for the [M+2H]²⁺ species at m/z 587.210 ±0.02 Da. The black trace displays the BPC of the fermentation supernatant. The grey area highlights the magnification area.*

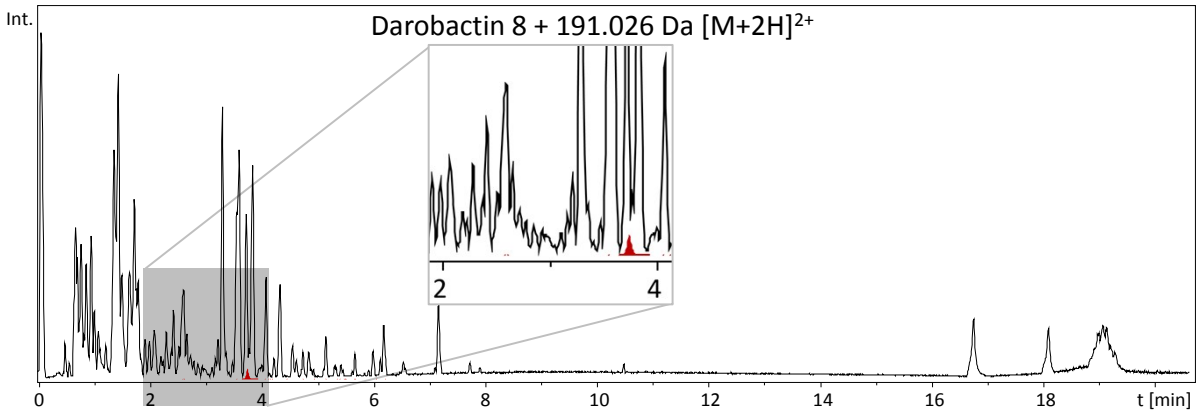

Suppl. Figure 12. Chromatogram of the E. coli *BL21 (DE3) pNOSO-darABCDE-8 culture supernatant. The red trace displays the darobactin 8 + 191.026 EIC for the [M+2H]²⁺ species at m/z 587.210 ±0.02 Da. The black trace displays the BPC of the fermentation supernatant. The grey area highlights the magnification area.*

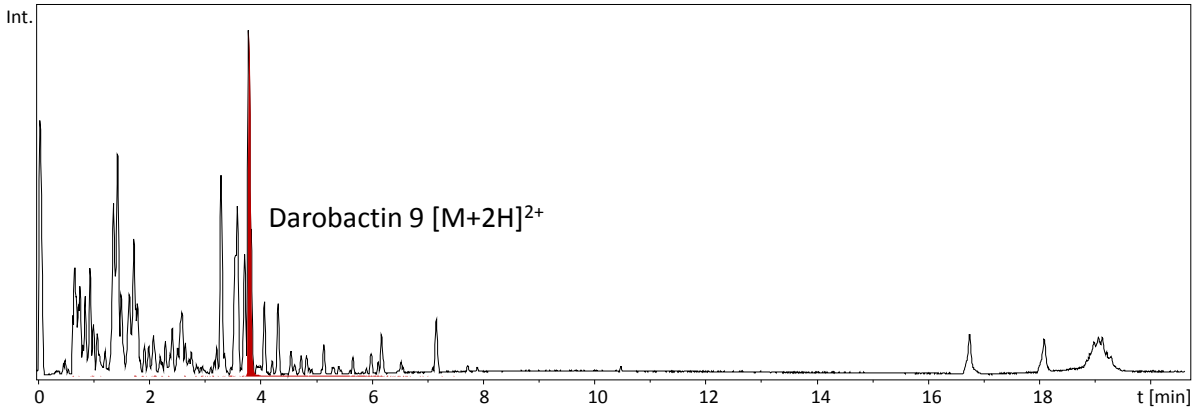

Suppl. Figure 13. Chromatogram of the E. coli *BL21 (DE3) pNOSO-darABCDE-9 culture supernatant. The red trace displays the darobactin 9 EIC for the [M+2H]²⁺ species at m/z 503.214 ±0.02 Da. The black trace displays the BPC of the fermentation supernatant.*

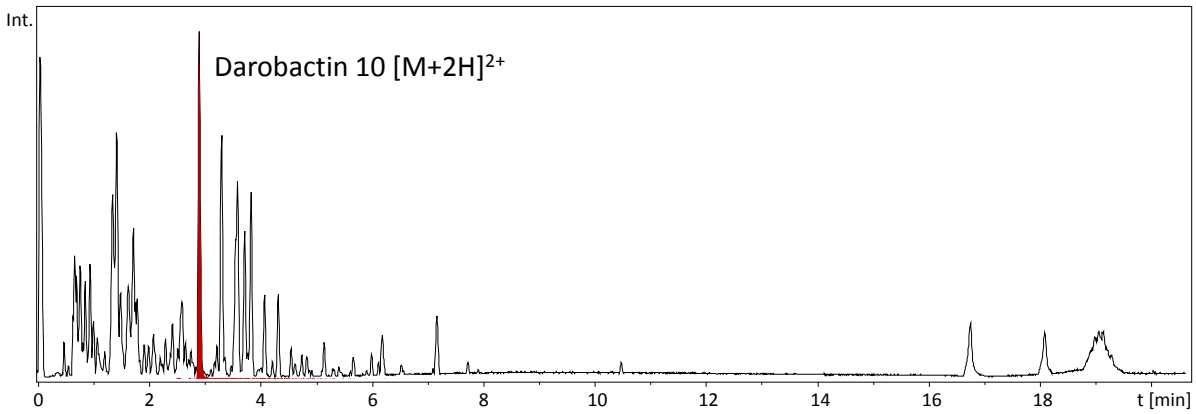

Suppl. Figure 14. Chromatogram of the E. coli *BL21 (DE3) pNOSO-darABCDE-10 culture supernatant. The red trace displays the darobactin 10 EIC for the $[M+2H]^{2+}$ species at m/z 491.706 ±0.02 Da. The black trace displays the BPC of the fermentation supernatant.*

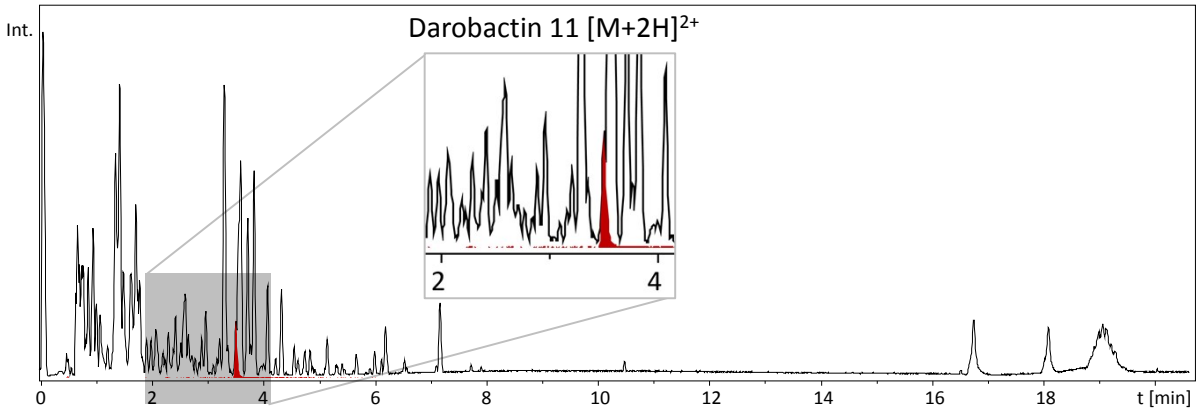

Suppl. Figure 15. Chromatogram of the E. coli *BL21 (DE3) pNOSO-darABCDE-11 culture supernatant. The red trace displays the darobactin 11 EIC for the $[M+2H]^{2+}$ species at m/z 490.717 ±0.02 Da. The black trace displays the BPC of the fermentation supernatant. The grey area highlights the magnification area.*

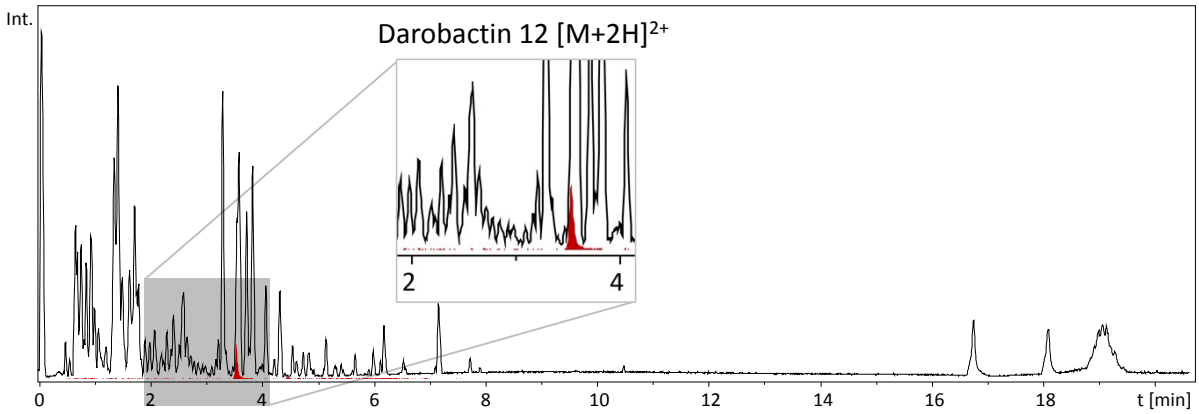

Suppl. Figure 16. Chromatogram of the E. coli *BL21 (DE3) pNOSO-darABCDE-12 culture supernatant. The red trace displays the darobactin 12 EIC for the $[M+2H]^{2+}$ species at m/z 477.211 ±0.02 Da. The black trace displays the BPC of the fermentation supernatant. The grey area highlights the magnification area.*

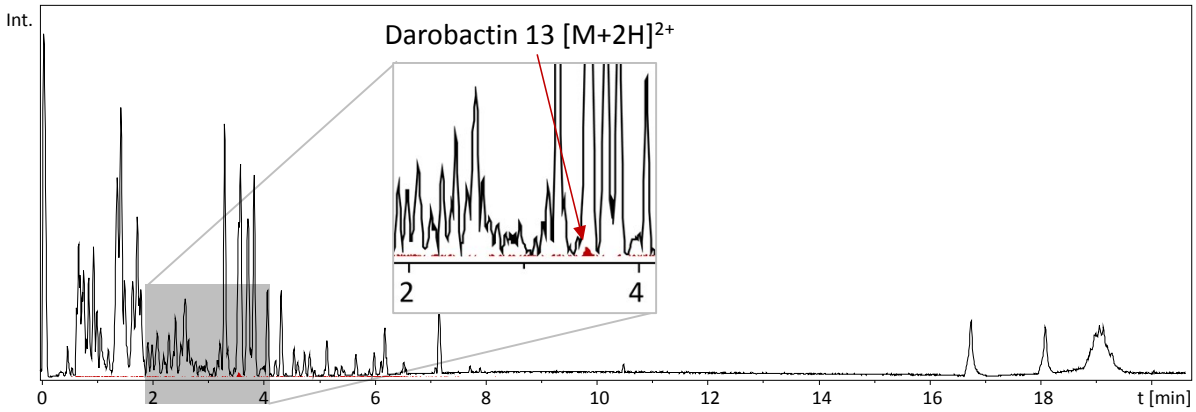

Suppl. Figure 17. Chromatogram of the E. coli *BL21 (DE3) pNOSO-darABCDE-13 culture supernatant. The red trace displays the darobactin 13 EIC for the $[M+2H]^{2+}$ species at m/z 462.206 ±0.02 Da. The black trace displays the BPC of the fermentation supernatant. The grey area highlights the magnification area and the red arrow points towards the darobactin 13 EIC peak.*

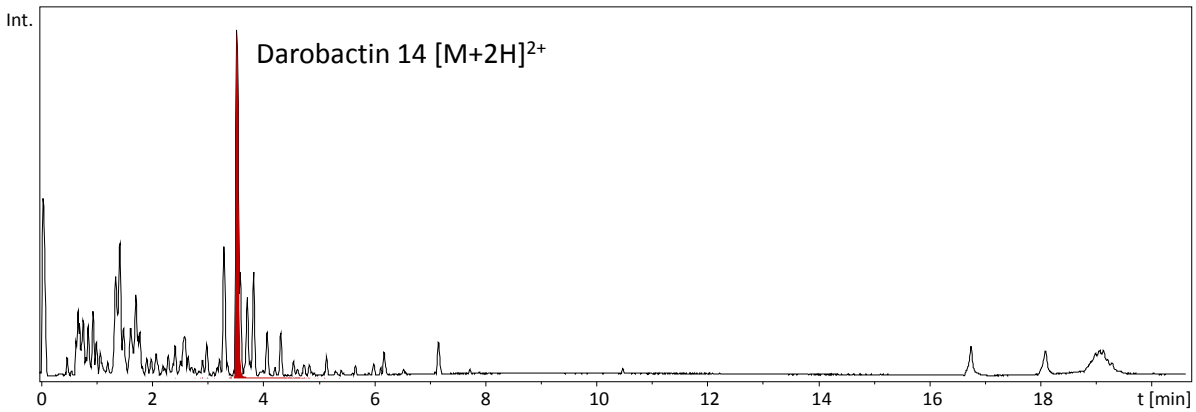

Suppl. Figure 18. Chromatogram of the E. coli *BL21 (DE3) pNOSO-darABCDE-14 culture supernatant. The red trace displays the darobactin 14 EIC for the $[M+2H]^{2+}$ species at m/z 475.712 ±0.02 Da. The black trace displays the BPC of the fermentation supernatant.*

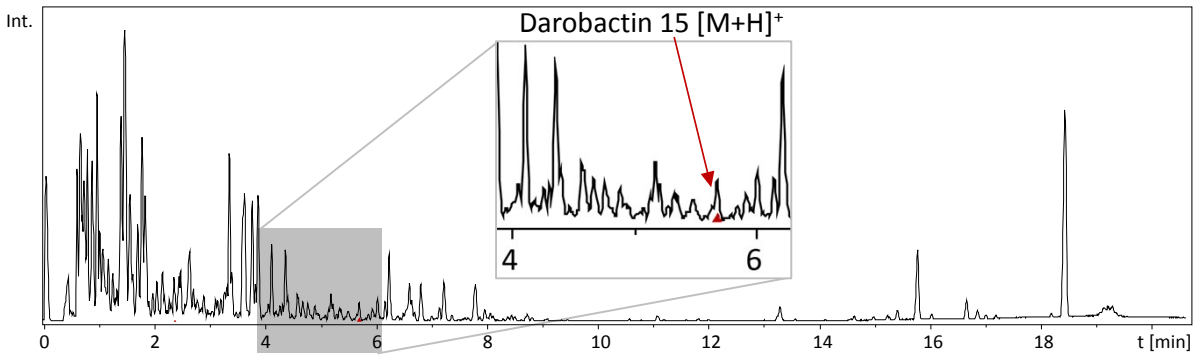

Suppl. Figure 19. Chromatogram of the E. coli *BL21 (DE3) pNOSO-darABCDE-15 culture supernatant. The red trace displays the darobactin 15 EIC for the $[M+H]^{+}$ species at m/z 909.351 ±0.02 Da. The black trace displays the BPC of the fermentation supernatant. The grey area highlights the magnification area and the red arrow points towards the darobactin 15 EIC peak.*

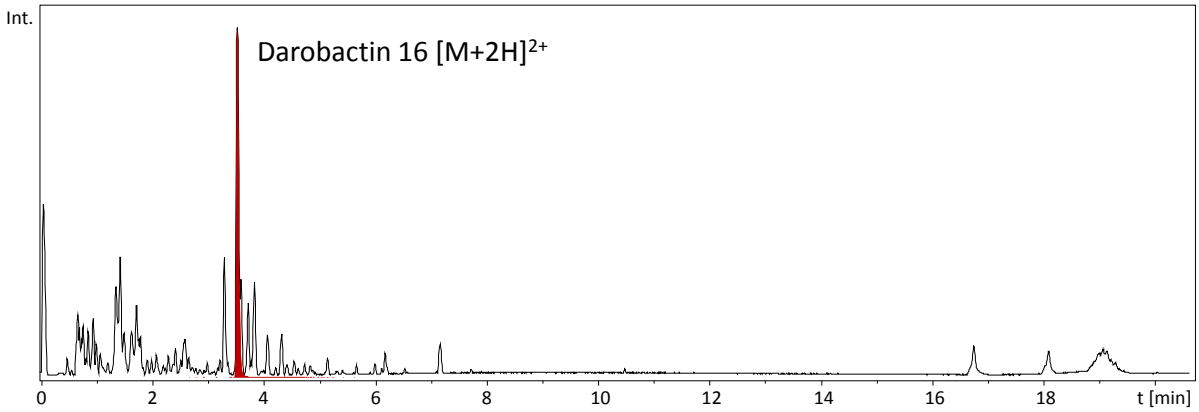

Suppl. Figure 20. Chromatogram of the E. coli *BL21 (DE3) pNOSO-darABCDE-16 culture supernatant. The red trace displays the darobactin 16 EIC for the $[M+2H]^{2+}$ species at m/z 475.712 ±0.02 Da. The black trace displays the BPC of the fermentation supernatant.*

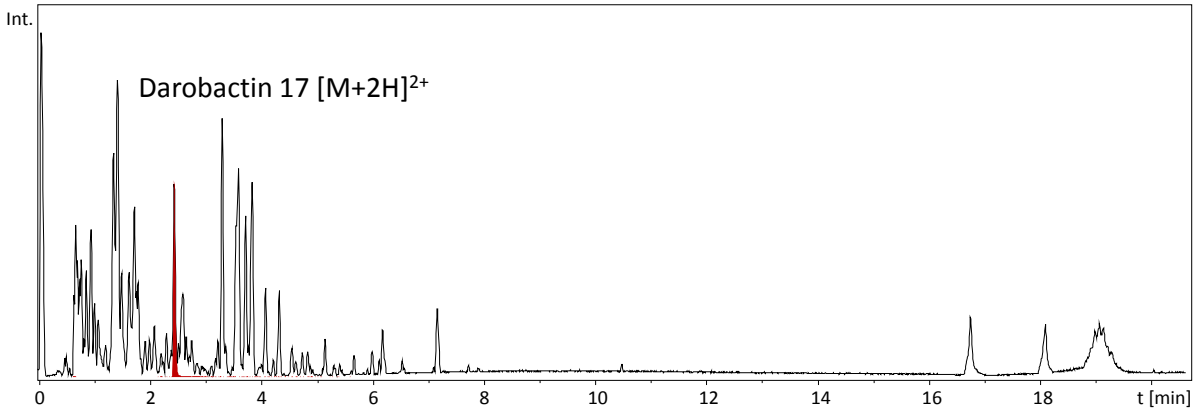

Suppl. Figure 21. Chromatogram of the E. coli *BL21 (DE3) pNOSO-darABCDE-17 culture supernatant. The red trace displays the darobactin 17 EIC for the $[M+2H]^{2+}$ species at m/z 445.693 ±0.02 Da. The black trace displays the BPC of the fermentation supernatant.*

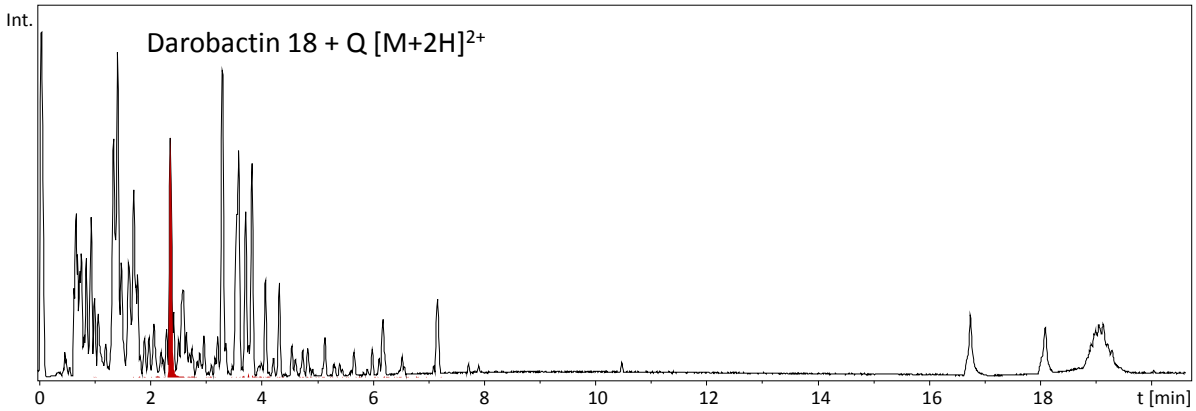

Suppl. Figure 22. Chromatogram of the E. coli *BL21 (DE3) pNOSO-darABCDE-18 culture supernatant. The red trace displays the darobactin 18 + Q EIC for the $[M+2H]^{2+}$ species at m/z 474.204 ±0.02 Da. The black trace displays the BPC of the fermentation supernatant.*

MS^2 spectral networking

All supporting GNPS clustering data to search for darobactins with unexpected precursor masses were created based on exported .mzML files from the uHPLC-$HRMS^2$ chromatograms using the parameters specified in the experimental section of the main text. The MS^2 chromatograms were exported containing all MS^2 data as an .mzML data file and uploaded to the GNPS server at University of California San Diego via FileZilla FTP upload to ftp:// ccms-ftp01.ucsd.edu and all acquired SPL MS^2 spectra are used for spectral network creation.[10] A molecular network was created using the online workflow at GNPS. The data were filtered by removing all MS^2 peaks within +/- 4 Da of the precursor m/z. MS^2 spectra were window filtered by choosing only the top six peaks in the +/- 50 Da window throughout the spectrum. The data were subsequently clustered with a parent mass tolerance of 0.05 Da and a MS^2 fragment ion tolerance of 0.1 Da to create consensus spectra. Further, no spectra were discarded based on consensus spectra calculation. Subsequently, a network was created, in which edges were filtered to have a cosine score above 0.65 and more than four matched peaks. Further edges between two nodes were kept in the network if and only if each of the nodes appeared in each other's respective top 10 most similar nodes.[10] The dataset was downloaded from the server and subsequently visualised using Cytoscape 3.7.2. In the data set, we searched for MS^2 spectra that clustered to the MS^2 spectrum of darobactin A or other identified darobactins. Confirmation of the respective darobactin core structure was done by manual inspection of the MS^2 spectrum. Notably, the darobactins 6 and 8 that feature a mass shift of +191.026 and darobactin 18 that features an additional L-glutamine were uncovered using this spectral networking approach.

MS^2 spectra for every observed darobactin derivative for structure confirmation

In this section, we list all observed MS^2 spectra for the produced darobactin derivatives. Differences in intensity of the spectra that directly correlate to the number of visible fragment ions are due to the significant differences in the production titres observed among the darobactin derivatives. Darobactin MS^2 spectra always display a prominent, doubly charged $[M\text{-}H_2O+2H]^{2+}$ ion as well as characteristic 160.08 and 300.09 fragments used for identification. The only exception was observed for darobactin 15 displaying a singly charged $[M\text{-}H_2O+H]^{+}$ ion and only the characteristic 300.09 fragment ion.

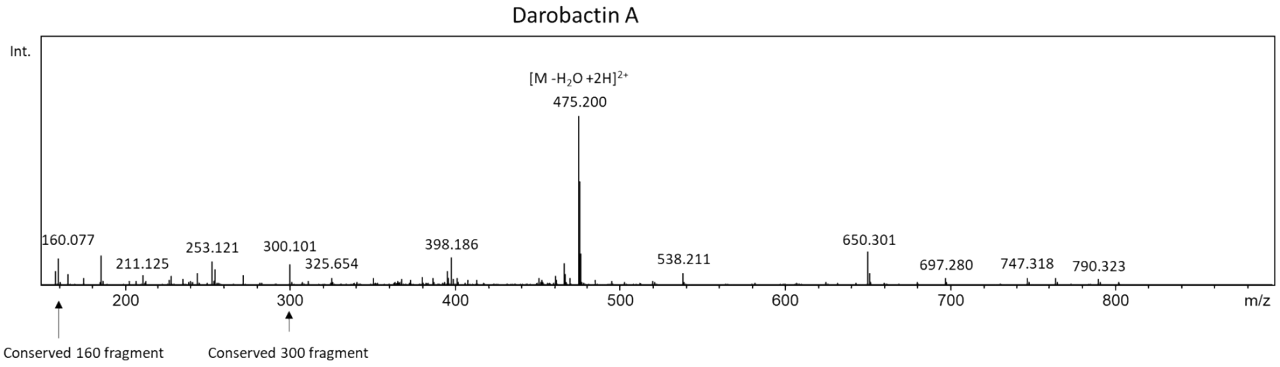

Suppl. Figure 23. MS² spectrum of darobactin A.

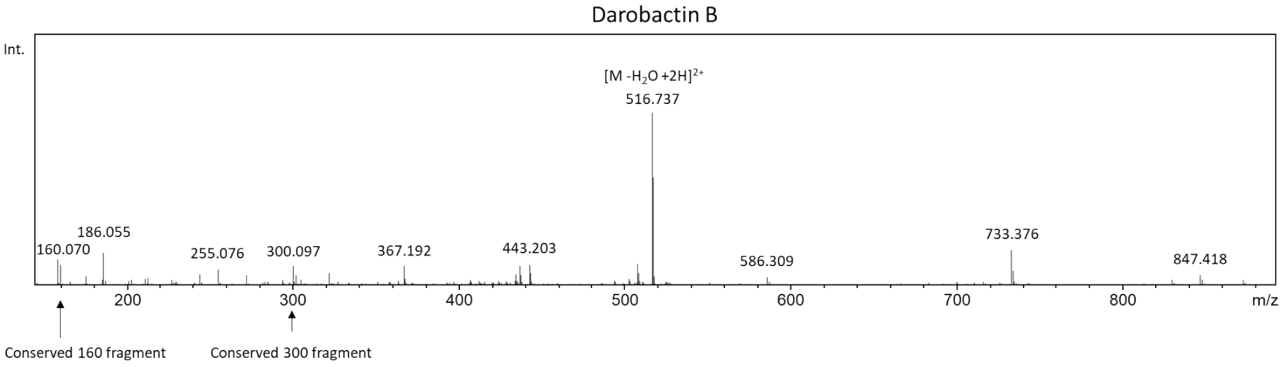

Suppl. Figure 24. MS² spectrum of darobactin B.

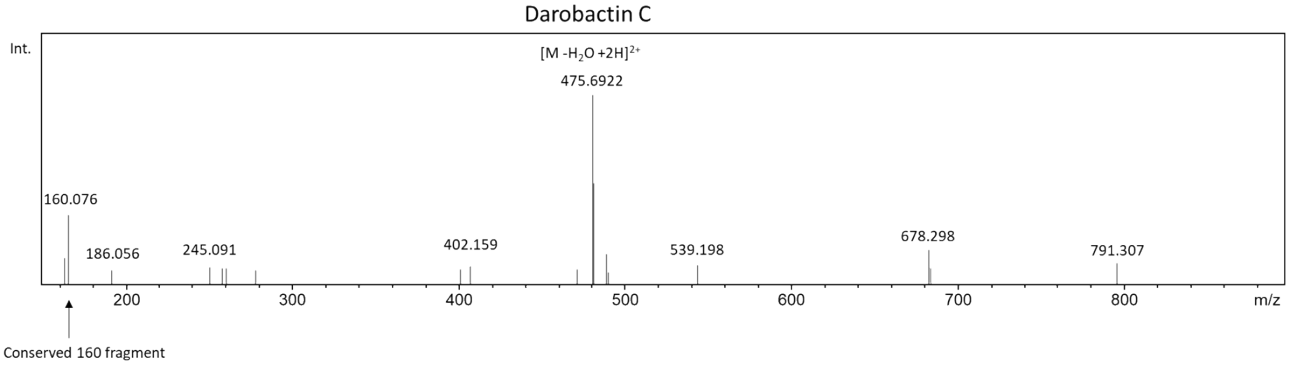

Suppl. Figure 25. MS² spectrum of darobactin C.

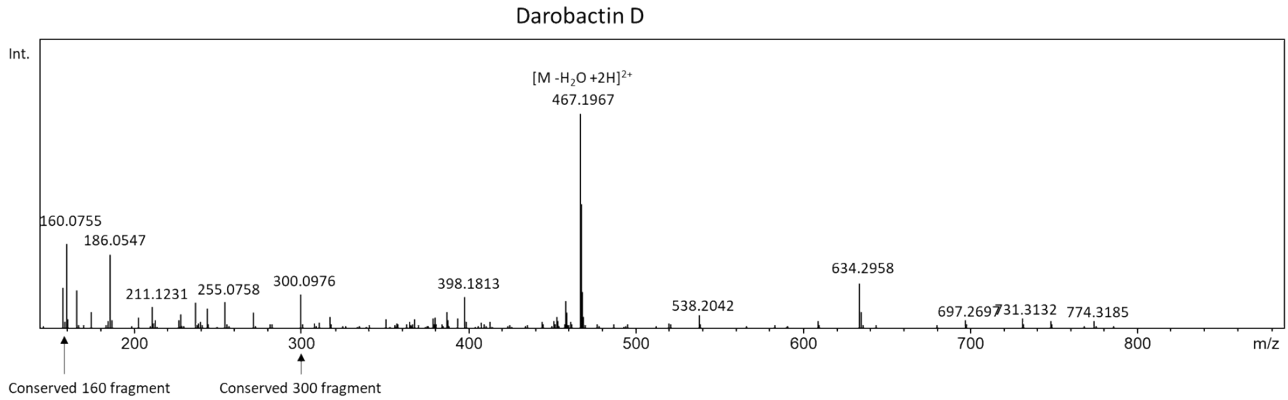

Suppl. Figure 26. MS² spectrum of darobactin D.

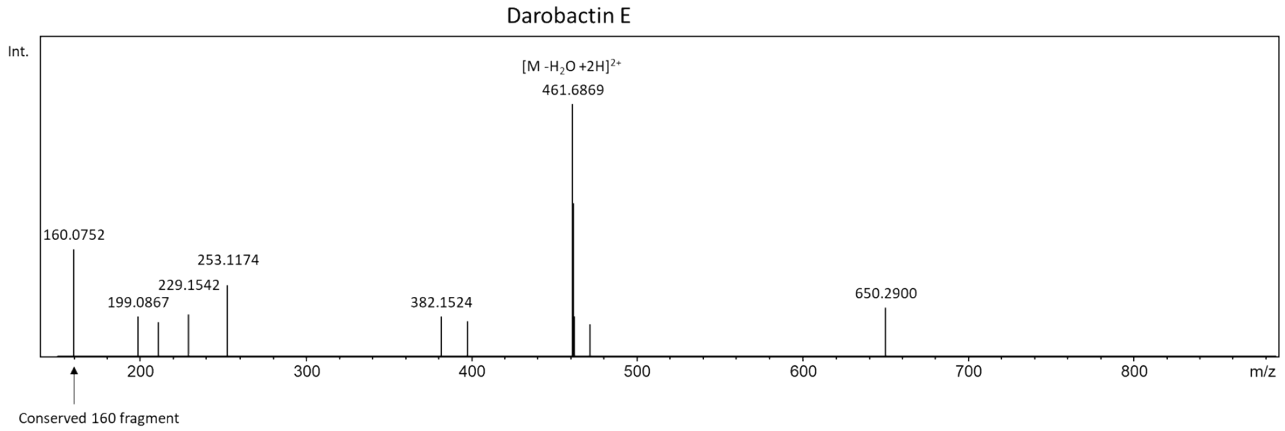

Suppl. Figure 27. MS² spectrum of darobactin E.

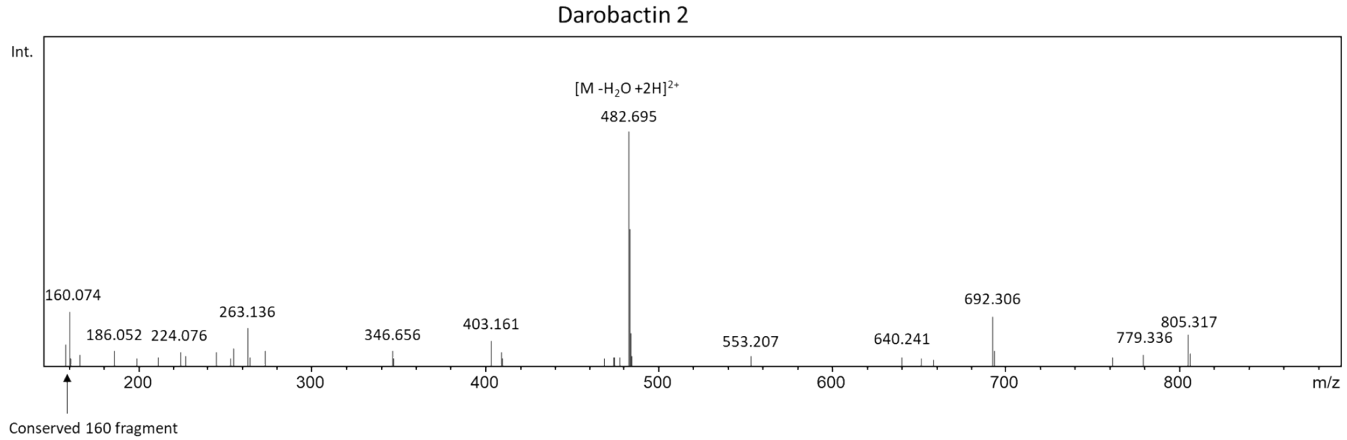

Suppl. Figure 28. MS² spectrum of darobactin 2.

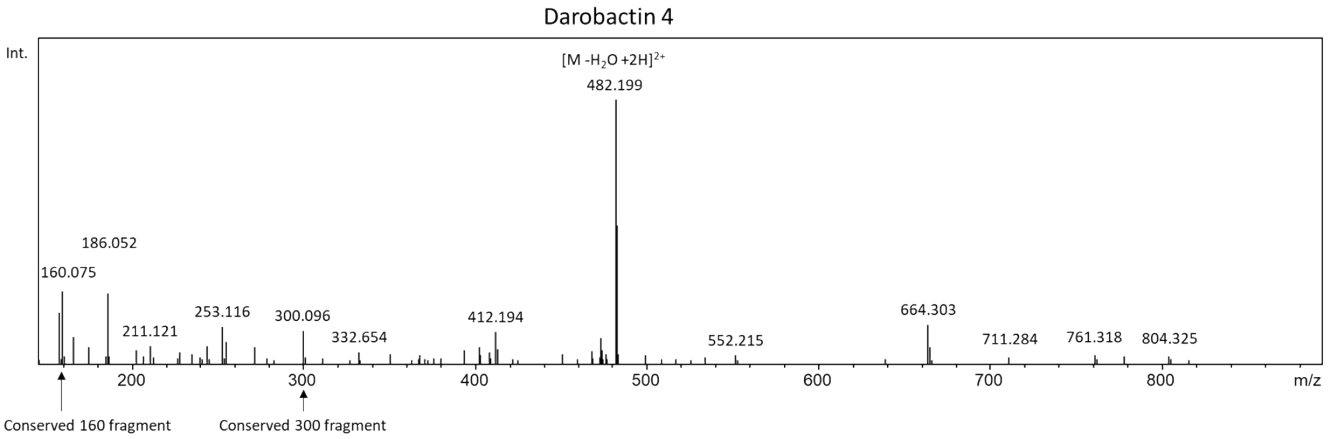

Suppl. Figure 29. MS² spectrum of darobactin 4.

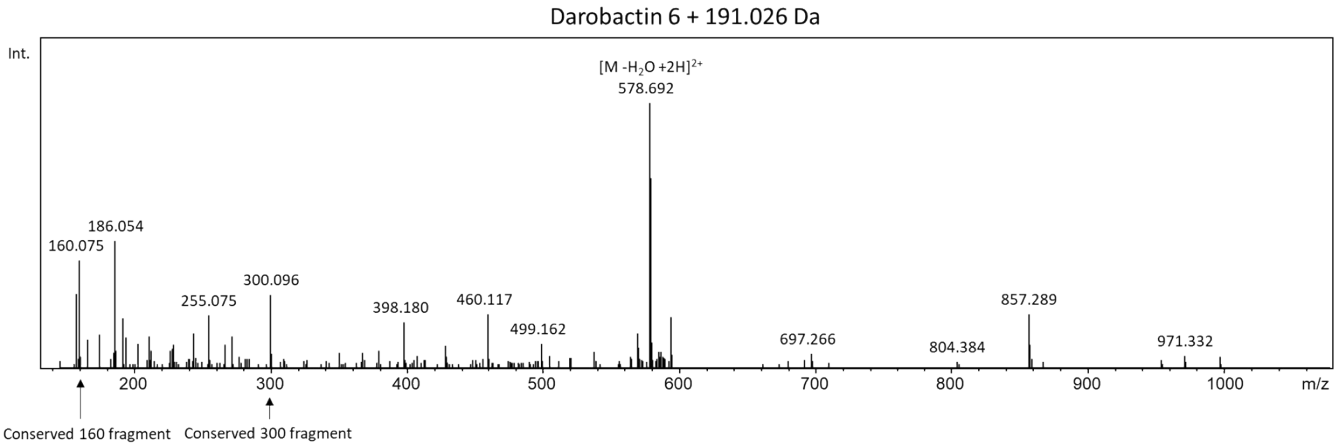

Suppl. Figure 30. MS² spectrum of darobactin 6 + the 191.026 Da adduct.

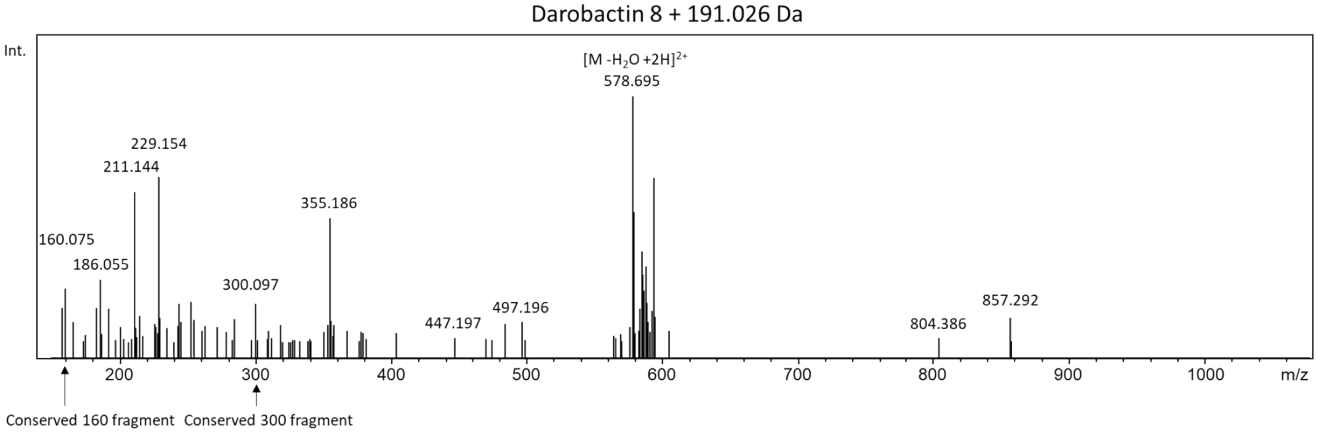

Suppl. Figure 31. MS² spectrum of darobactin 8 + the 191.026 Da adduct.

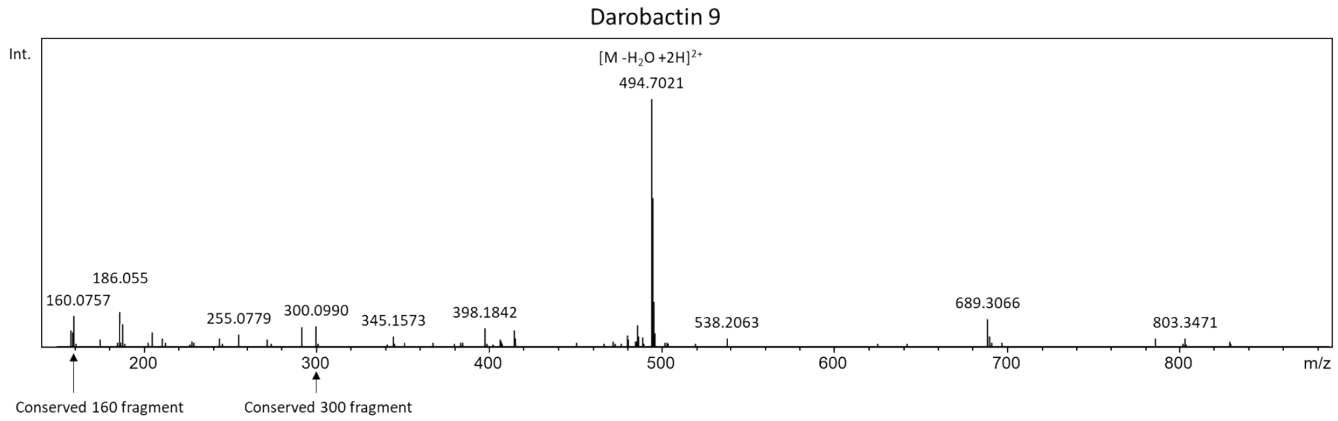

Suppl. Figure 32. MS² spectrum of darobactin 9.

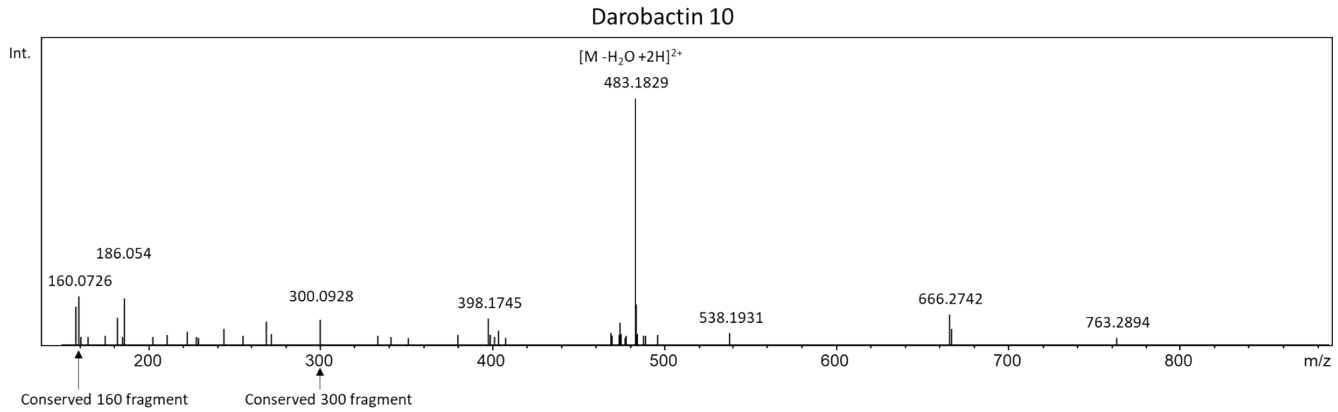

Suppl. Figure 33. MS² spectrum of darobactin 10.

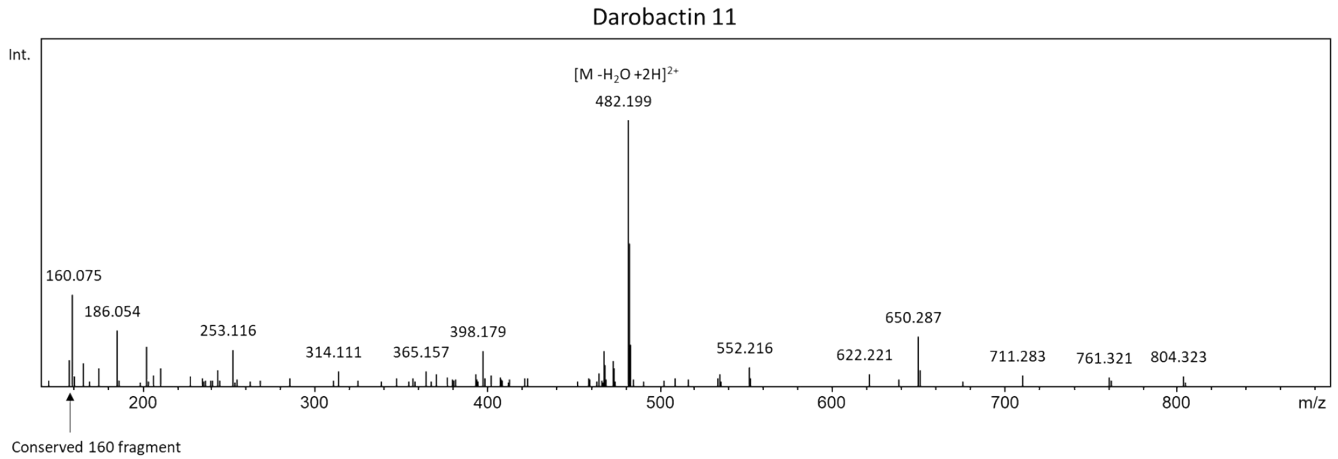

Suppl. Figure 34. MS² spectrum of darobactin 11.

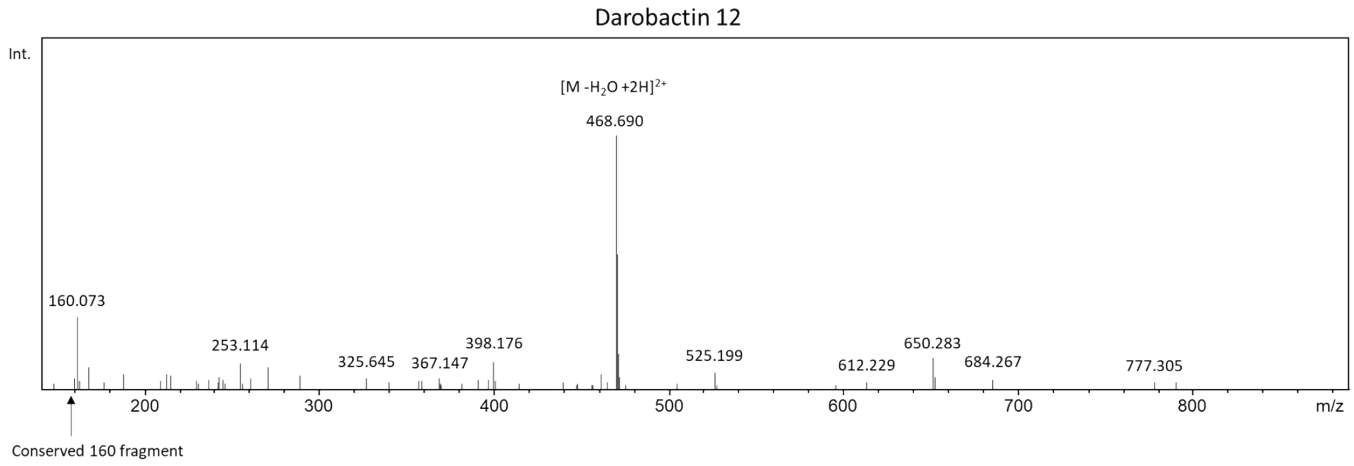

Suppl. Figure 35. MS² spectrum of darobactin 12.

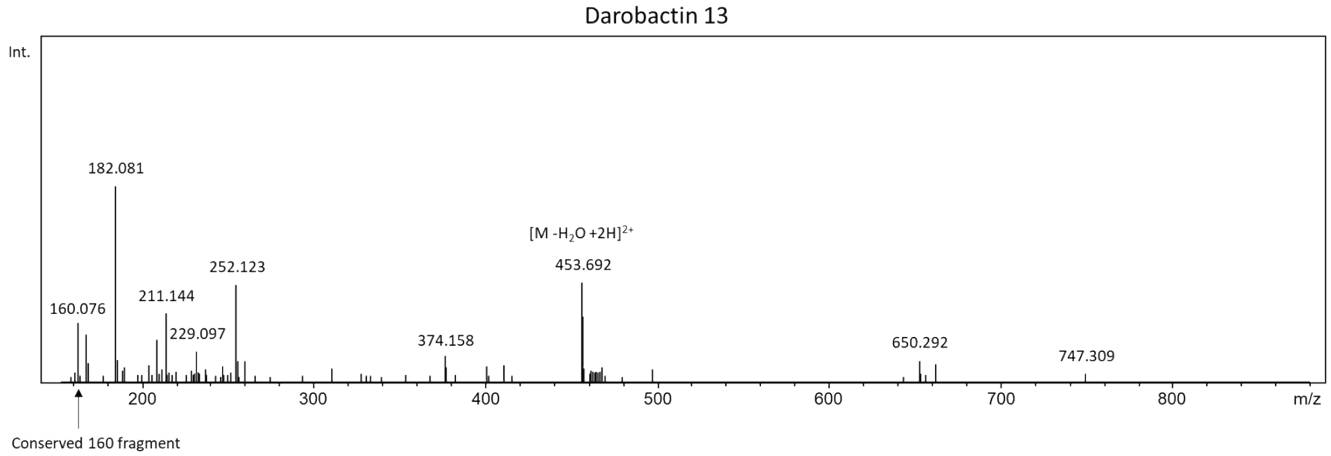

Suppl. Figure 36. MS² spectrum of darobactin 13.

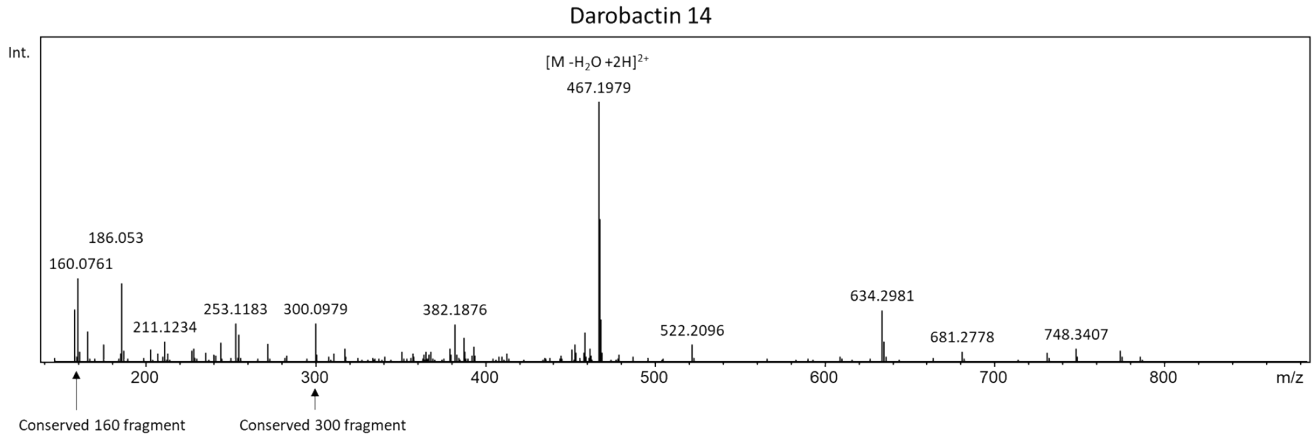

Suppl. Figure 37. MS² spectrum of darobactin 14.

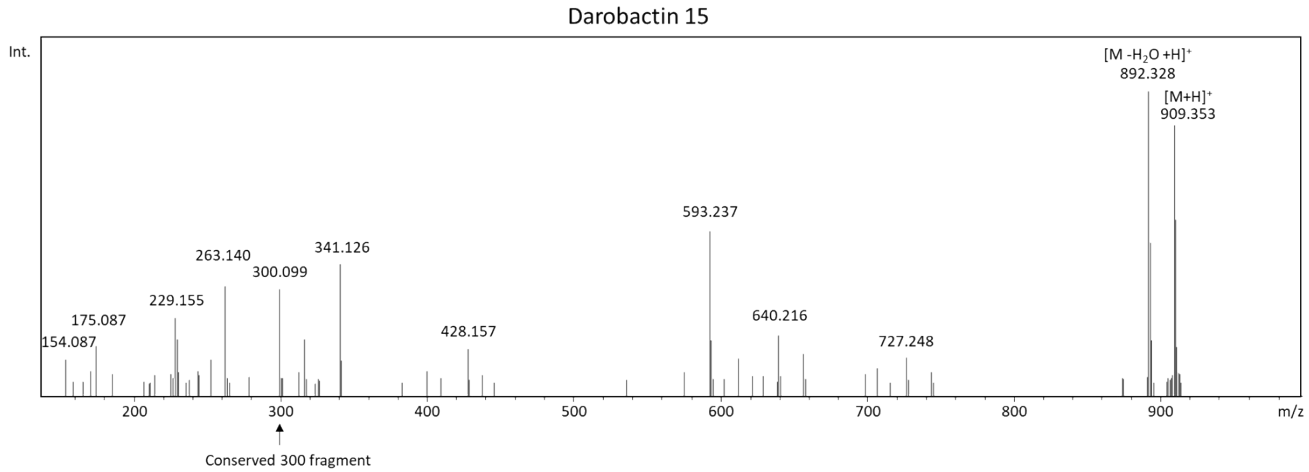

Suppl. Figure 38. MS² spectrum of darobactin 15.

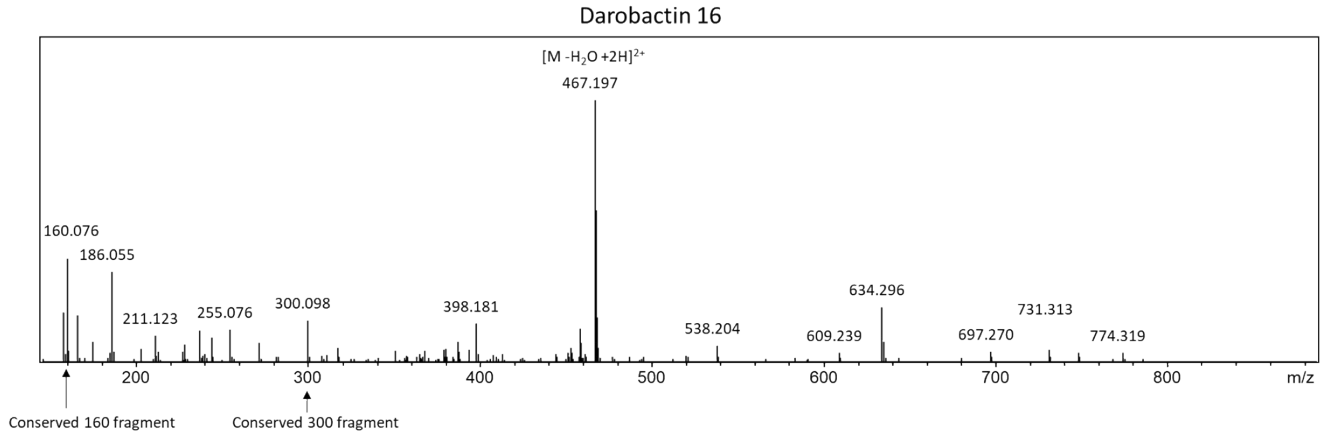

Suppl. Figure 39. MS² spectrum of darobactin 16.

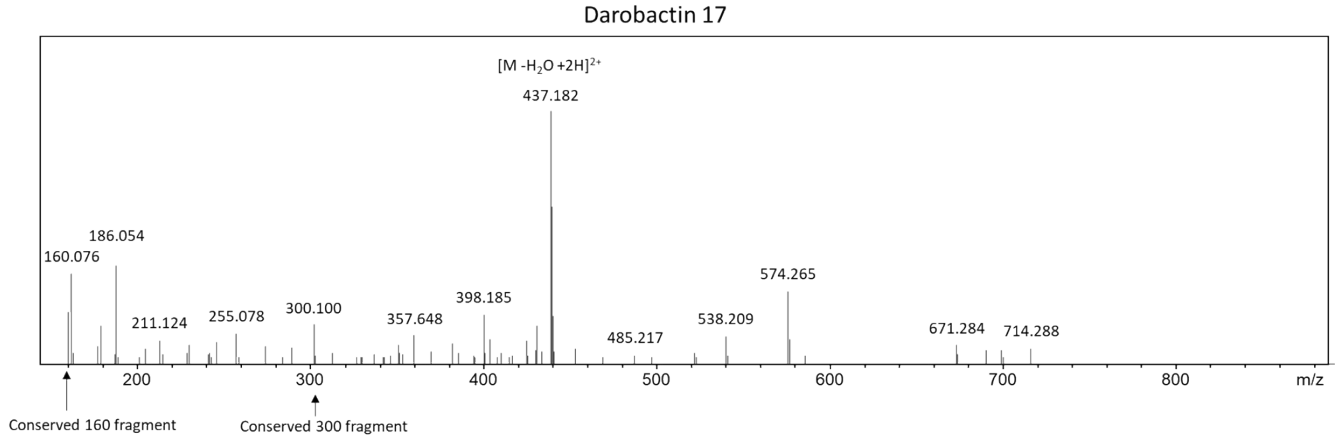

Suppl. Figure 40. MS² spectrum of darobactin 17.

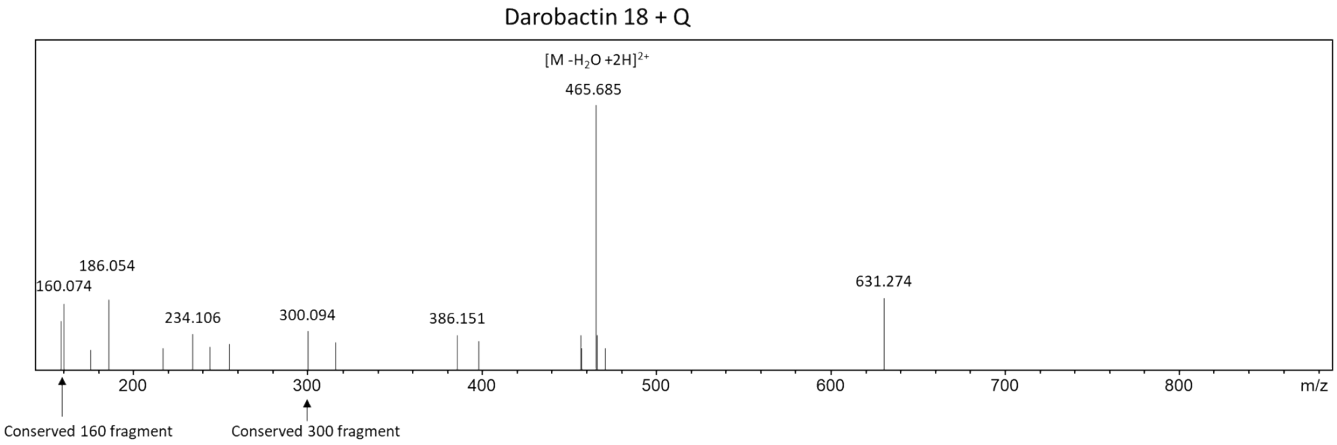

Suppl. Figure 41. MS² spectrum of darobactin 18 + L-glutamine from the follower peptide.

Evaluation of the relative minimal inhibitory concentration (MIC) of darobactin derivatives based on tested crude extracts

In order to determine the relative MIC of darobactin derivatives with respect to darobactin A, the supernatant of the fermentation broth from 50 mL screening cultures was collected after centrifugation at 7,750 x g for 10 min at 4 °C. Next, 10 % (v/v) XAD-16N resin was added with subsequent incubation for 2 h at room temperature and 180 rpm on an orbital shaker (Orbitron/Multitron, Infors HT). After passive sedimentation of the absorber resin, the supernatant was carefully decanted and the absorber resin was incubated in 80 % (v/v) MeOH/H_2O for 2 h at room temperature and shaking at 180 rpm. The crude extract was subsequently filtered using folded filter paper (8 – 12 µm pore size) and dried using a rotary evaporator. The dried extract was dissolved in 500 µL 50 % (v/v) MeOH in H_2O, resulting in a 100 x concentration factor, and was subsequently analysed using uHPLC-HRMS (described above) prior its use in MIC evaluation assay. For uHPLC-HRMS analysis, each extract was further diluted 1:5 in H_2O. The MS peak surface of each respective darobactin derivate was determined by automated peak integration using *Compass DataAnalysis* version 4.4 (Bruker Daltonics).

For MIC evaluation, 20 µL of the prepared extract were transferred into a well of the first row of a 96-well plate. After passive MeOH evaporation at room temperature, 70 µL Mueller-Hinton broth (MHB; 2 g/L beef infusion solids, 1.5 g/L starch, 17.5 g/L casein hydrolysates, final pH 7.4) or TSB medium were added to the remaining 5 µl concentrated extracts in the wells of row A, and 75 µL MHB medium or TSB medium were added into all wells. Starting from the extract/medium mixture in the first row, serial dilutions were prepared in corresponding subjacent rows of the 96-well plate (Suppl. Figure 42).

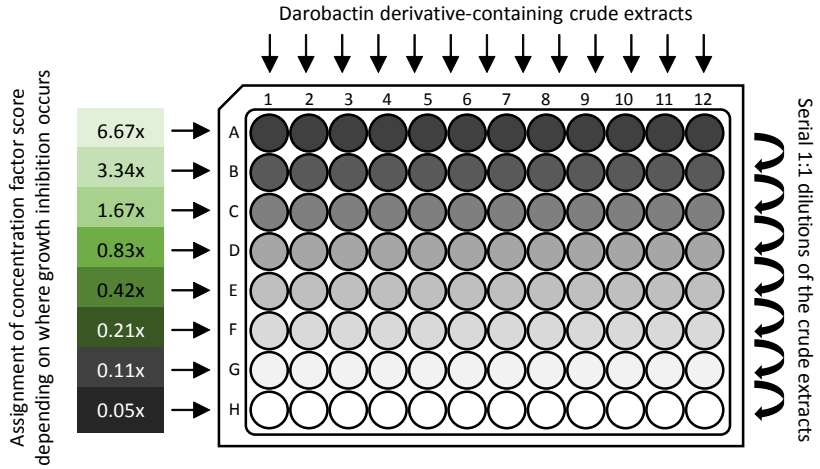

Suppl. Figure 42. The darobactin derivative-containing crude extracts (100x concentrated) were serially 1:1 diluted in a 96-well plate starting from well A (1:15 dilution) to well H (1:1,920 dilution). The concentration factor was calculated from the crude extract concentration divided by the dilution in the respective row. The well position, in which an activity of the compound against the strain was last (visually) detected, was assigned to the concentration factor score.

Next, bacterial cell suspensions of *Acinetobacter baumannii* DSM-30008, *Pseudomonas aeruginosa* PA01, *E. coli* ATCC25922 and *Klebsiella pneumoniae* DSM-30104 were prepared. Single colonies of the bacterial strains were suspended in 0.9 % (w/v) NaCl and McFarland was adjusted to 0.5. The bacterial suspension was diluted 1:100 in MHB (in case of *A. baumannii* DSM-30008, *P. aeruginosa* PA01 and *E. coli* ATCC25922) or TSB (*K. pneumoniae* DSM-30104) to achieve a final inoculum of approximately 10^6 colony-forming units (CFU)/mL. 75 µL of these suspensions were added to each well of the 96-well plates containing the extracts in serial dilution (final inoculum of 5 x 10^5 CFU/mL). Growth inhibition was assessed after 24 h incubation under static conditions at either 30°C (*A. baumannii*) or 37°C (all others). MIC was evaluated visually by determining the dilution factor (row A = 1:15; row B = 1:30; etc.) where visible growth of the respective strain was no longer observed. Finally, the concentration facor of the tested extract was calculated by division of the concentration (100x caused by the extraction process) by the dilution factor in which visible growth of the respective strain was no longer observed. For example, if the darobactin derivative-containing crude extract in column 1 (see Suppl. Figure 42) resulted in growth inhibition of the respective strain from wells A1 to E1, but not anymore in F1, we assigned the concentration factor score 0.42x to the darobactin derivative. If the darobactin derivative-containing crude extract in column 2 resulted in growth inhibition only from wells A2 to B2, but not anymore in C2, we assigned the concentration factor score 3.34x, meaning that the crude extract in column 1 showed stronger antibacterial activity (assuming that the compound concentration is similar).

Determination of the MS peak area under curve (AUC) ratio

To calculate the relative quantity of each darobactin derivative compared to darobactin A in the crude extracts (crude extract preparation is described in previous section), the MS peak surface areas of the respective $[M+2H]^{2+}$ EICs were determined by automated peak integration using *Compass Data Analysis* version 4.4 (Bruker Daltonics). Next, the AUC of each derivative was divided by the AUC of the darobactin A peak. Raw data and calculations are supplied in the Source data file.

Large scale fermentation of darobactins A and 9 for purification

Large scale fermentation of *E. coli* BL21 (DE3) pNOSO-darABCDE and *E. coli* BL21 (DE3) pNOSO-darABCDE-9 in 6 x 1 L FM medium (supplemented with 1 mg/L vitamin B_{12} after medium sterilization) was performed in 5 L baffled shake flasks for 3 days at 30 °C and 160 rpm on an orbital shaker (Orbitron/Multitron, Infors HT). Each 1 L production culture was inoculated with 50 mL of an LB seed culture grown overnight in a 300 mL unbaffled shaking flask at 30 °C and 180 rpm. After large scale fermentation, the cells were separated from the supernatant by centrifugation on an Avanti J-26 XP centrifuge (Beckman Coulter, Brea, California (US)) with the JLA 8.1 rotor at 6,000 rcf. XAD-16N resin was added to the clarified supernatant and the mixture was shaken on an orbital shaker (Orbitron/Multitron, Infors HT) at 160 rpm for 2 h. This extraction step was performed two to three times and the combined resin subsequently extracted using 3 x 500 mL of 80% MeOH in H_2O. After solvent evaporation using a rotary evaporator, the dried extract was redissolved in H_2O and the purity was analysed by uHPLC-HRMS.

Purification of darobactins A and 9

As both darobactins, darobactin A and darobactin 9, show similar behavior in chromatographic separation, they can be purified using the same set of methods. The dried extract (extract preparation described in the section before) was taken up in a minimum of milliQ H_2O and purified on a preparative Autopurifier HPLC-MS (Waters Corp.) system with H_2O and ACN (+0.1 % FA) on a XBridge C_{18} column (5 µm, 19x150 mm; Waters Corp.) at a flow rate of 25 mL/min going from 2-25% ACN in 24 min followed by a ramp to a flushing step at 95% ACN and a ramp back to the initial conditions. Darobactins were detected by their respective mass signals of 483.70 $[M+2H]^{2+}$ and 503.21 $[M+2H]^{2+}$ for darobactins A and 9, respectively, on the built-in single quadrupole mass analyzer. Darobactin A eluted at 10 min and darobactin 9 eluted at 12 min. The darobactin-containing fractions were collected and dried using a

rotary evaporator. The samples were subsequently dissolved in a minimum of milliQ H_2O and purified on the same preparative Autopurifier HPLC-MS system with H_2O and ACN (+0.1 % FA) on a Kinetex Biphenyl column (5 µm, 19x250 mm; Phenomenex Inc., Torrance, California (US)) at a flow rate of 25 mL/min going from 2-20% ACN in 24 min followed by a ramp to a flushing step at 95% ACN and a ramp back to the initial conditions. Darobactin A eluted at 15 min and darobactin 9 eluted at 21 min. The third step of the purification of darobactins A and 9 was carried out using an Ultimate 3000 SDLC low pressure gradient system (Dionex) equipped with an Acquity CSH Phenyl-hexyl column (250x10mm 5µm; Waters Corp.). The eluents were H_2O + 0.1% FA as A and ACN + 0.1% FA as B, at a flow rate of 5 mL/min and a column thermostatic at 45 °C. The darobactins were detected by UV absorption at 280 nm and the purification was done by time-dependent fraction collection. The separation was started with a plateau at 2% B for 2 min followed by a ramp to 15% B during 20 min and a ramp to 95% B during 1 min. The A content was kept at 5% B for 2 min. The B content was ramped back to starting conditions during 30 seconds and the column was re-equilibrated for 2 min. Darobactin A elutes at 14.8 min and darobactin 9 elutes at 16.7 min. After evaporation, the darobactins were obtained as pale yellowish amorphous solids. After purification, uHPLC-HRMS analysis shows a single peak with an exact mass of 483.701 $[M+2H]^{2+}$ and 503.212 $[M+2H]^{2+}$ for darobactins A and 9, respectively. The purity of the isolated compounds was assessed on the one hand by uHPLC-HRMS as judged from the MS trace as well as the UV trace from 200 to 600 nm. In addition to that, the compounds purity was provided by the 'cleanliness' meaning the absence of non-darobactin signals in the NMR spectrum.

Structure elucidation of darobactins A and 9

1D and 2D NMR data used for the structure elucidation of darobactin 9 were acquired in a 2:1 mixture of H_2O-d_2 acetonitrile-d_3-containing 2 % formic acid-d_2 on an UltraShield 500 spectrometer (Bruker Daltonics) equipped with a 5 mm TCI cryoprobe (^1H at 500 MHz, ^{13}C at 125 MHz). The spectra were recorded at 45 °C and calibrated on the remaining non-deuterated acetonitrile signals. All observed chemical shift values (δ) are given in ppm and the coupling constant values (J) in Hz. Standard pulse programs were used for HMBC, HSQC, and gCOSY experiments. HMBC experiments were optimized for $^{2,3}J_{C\text{-}H}$ = 6 Hz. The NMR signals were grouped in the tables below and correspond to the numbering in the schemes corresponding to every table. All structure formulae devised by NMR will be made publicly available under their corresponding name in NPAtlas[11] upon acceptance of the manuscript.

Quantification of darobactins A and 9 production

The quantification of darobactin A in the heterologous producers *E. coli* BL21 (DE3) pNOSO-darABCDE, *E. coli* BL21 (DE3) pNOSO-darACDE, *E. coli* BL21 (DE3) pNOSO-darABDE and *E. coli* BL21 (DE3) pNOSO-darABCE, as well as the quantification of darobactin 9 in *E. coli* BL21 (DE3) pNOSO-darABCDE-9 was done using an amaZon speed 3D ion trap MS system (Bruker Daltonics) with an Apollo II ESI source. The LC system, column and settings as well as the ESI source settings were identical as described above. We measured darobactin A and darobactin 9 standard solutions with concentrations of 1000 mg/mL, 500 mg/mL, 250 mg/mL, 125 mg/mL, 62.5 mg/mL, 31.25 mg/mL, 15.63 mg/mL, 7.81 mg/mL, 3.91 mg/mL, 1.95 mg/mL, 0.98 mg/mL. Solutions for each concentration were prepared three times and measured two times. The EICs m/z 483.70 $[M+2H]^{2+}$ as peak surface of darobactin A and m/z 503.20 $[M+2H]^{2+}$ as peak surface area of darobactin 9 were determined by automated peak integration using *Compass Data Analysis* version 4.4 (Bruker Daltonics). All standard solutions were measured in duplicates to ensure reproducibility. The linear range of the setup was experimentally determined to be between 0.98 mg/mL and 62.5 mg/mL for darobactin A and 0.98 mg/mL and 15.63 mg/mL for darobactin 9. The mean values of each measurement were used to construct a regression line that was used to calculate the quantity of darobactin A and darobactin 9 in the cultivation extract. Source data are supplied in the Source data file.

Evaluation of MICs of pure darobactins A and 9

All strains were handled according to standard procedures and were purchased from the German Collection of Microorganisms and Cell Cultures (DSMZ), the American Type Culture Collection (ATCC) and the Coli Genetic Stock Centre (CGSC; Keio collection).[12] *E. coli* BL21 (DE3) is part of our internal strain collection and *P. aeruginosa* strains were kindly provided by Prof. D. S. Häußler. The clinical isolates were kindly provided by Dr. P. Chhatwal, L. Knegendorf, and Prof. Dr. D. Schlüter from Hannover Medical School. Darobactins were prepared as DMSO stock solutions and MICs were established using microbroth dilution as described elsewhere.[13] In brief, serial dilutions of compounds (0.03-64 µg/mL) in MHB were prepared in sterile 96-well plates. Bacterial suspensions in MHB were added to achieve a final inoculum of 5×10^5 CFU/mL. Depending on the growth requirements of tested bacteria, the plates were incubated for 24 h at either 30 °C or 37 °C. MICs were defined as lowest concentration of antibiotic at which no visible growth was observed.

Sample information and antibiograms of clinical bacterial isolates

Suppl. Table 8. Sampling data of used clinical isolates. [a] 3MRGN: multi-resistant gram-negative bacteria, non-susceptible to three specific groups of antibiotics; ESBL: Extended spectrum β-lactamases.

Strain ID	**Sample type**	**Month/year of isolation**	**Resistance phenotype[a]**
E. coli ECO24	Midstream urine	02/2020	Quinolone resistant
E. coli ECO25	Permanent catheter urine	02/2020	3MRGN
K. pneumoniae KPN12	Permanent catheter urine	02/2020	3MRGN
K. pneumoniae KPN19	Midstream urine	02/2020	3MRGN
K. pneumoniae KPN62	Sputum	03/2020	ESBL

Suppl. Table 9. Antibiogram of clinical isolates. [a] R: resistant (shown in red); I: intermediate (shown in yellow); S: sensitive (shown in green).

	ECO24	**ECO25**	**KPN12**	**KPN19**	**KPN62**
Ampicillin	R	R	R	R	R
Ampicillin-Sulbactam	R	R	R	R	R
Piperacillin / Sulbactam		R	R	R	R
Piperacillin-Tazobactam	S	I	I	R	I
Cefuroxim	I	R	R	R	R
Cefuroxim-Axetil	S	R	R	R	R
Cefpodoxim	S	R	R	R	R
Ceftriaxon	S	R	R	R	R
Cefotaxim	S	R	R	R	R
Ceftazidim	S	R	R	R	R
Gentamicin	R	R	I	R	I
Fosfomycin	S	S	R	R	
Nitrofurantoin	S	S			
Levofloxacin	R	R	I	R	S
Ciprofloxacin	R	R	R	R	S
Moxifloxacin	R	R	R	R	S
Meropenem	S	S	S	I	S
Ertapenem					S
Cotrimoxazol	R	S	R	R	S

NMR data for darobactin 9

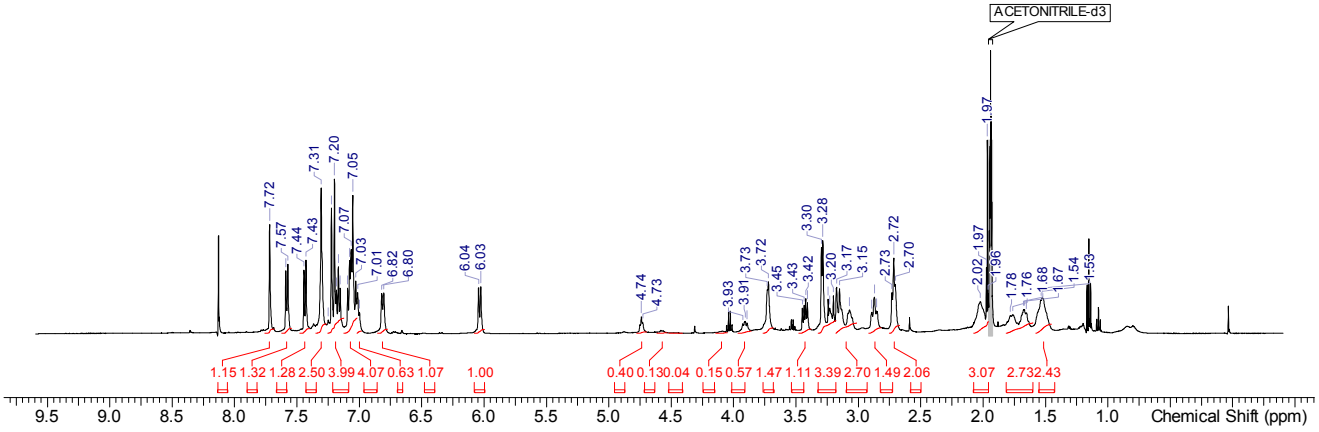

Suppl. Figure 43.Water suppressed ^{1}H spectrum of darobactin 9 in a 2:1 mixture of H_2O-d_2 acetonitrile-d_3-containing 2 % formic acid-d_2 at 45 °C and 500 MHz.

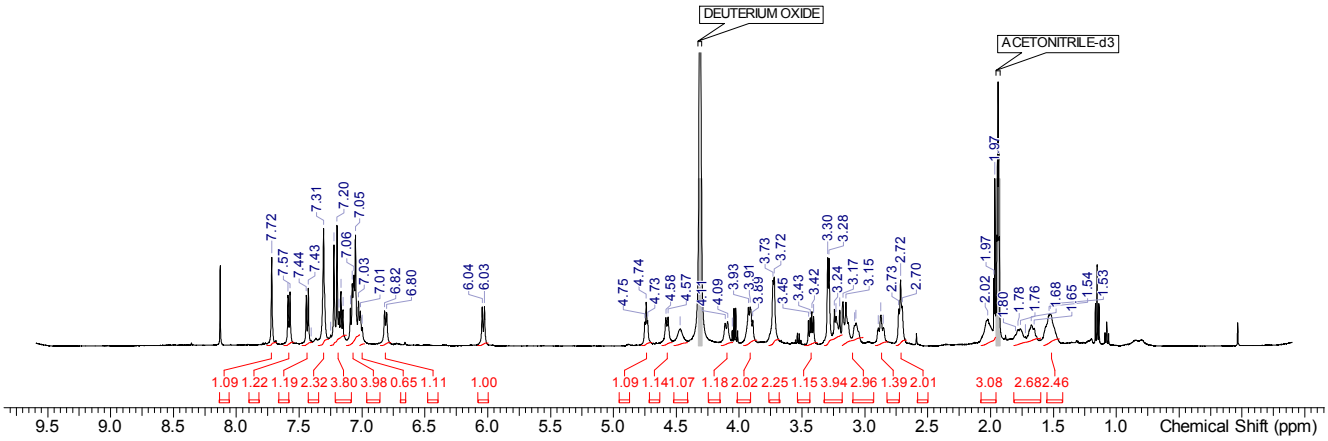

Suppl. Figure 44. ^{1}H spectrum of darobactin 9 in a 2:1 mixture of H_2O-d_2 acetonitrile-d_3-containing 2 % formic acid-d_2 at 45 °C and 500 MHz.

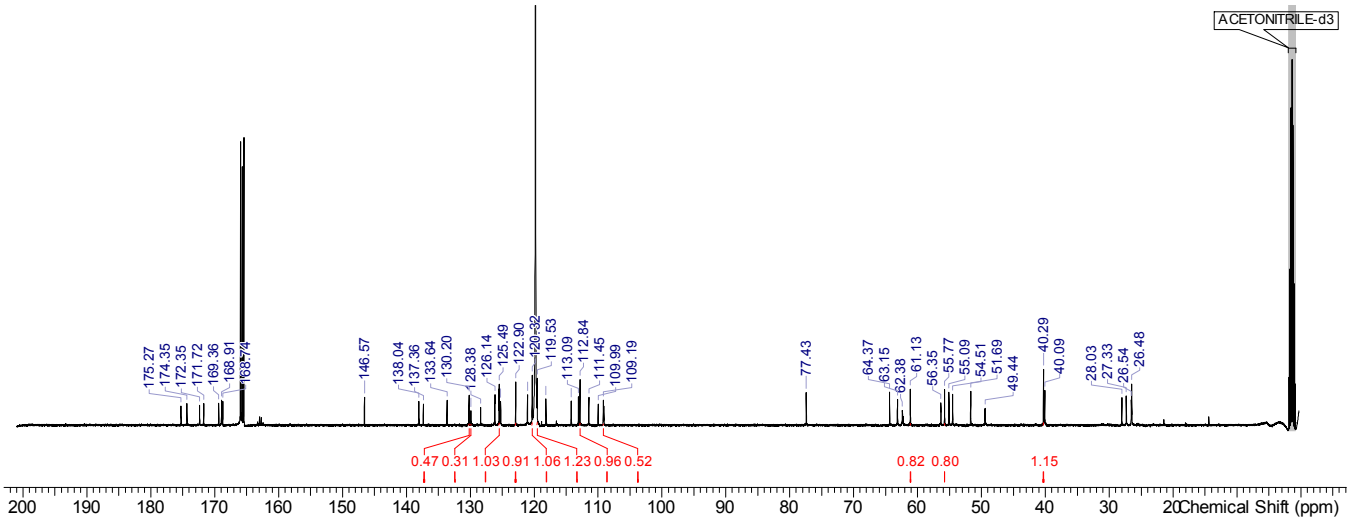

Suppl. Figure 45. ^{13}C spectrum of darobactin 9 in a 2:1 mixture of H_2O-d_2 acetonitrile-d_3-containing 2 % formic acid-d_2 at 45 °C and 125 MHz.

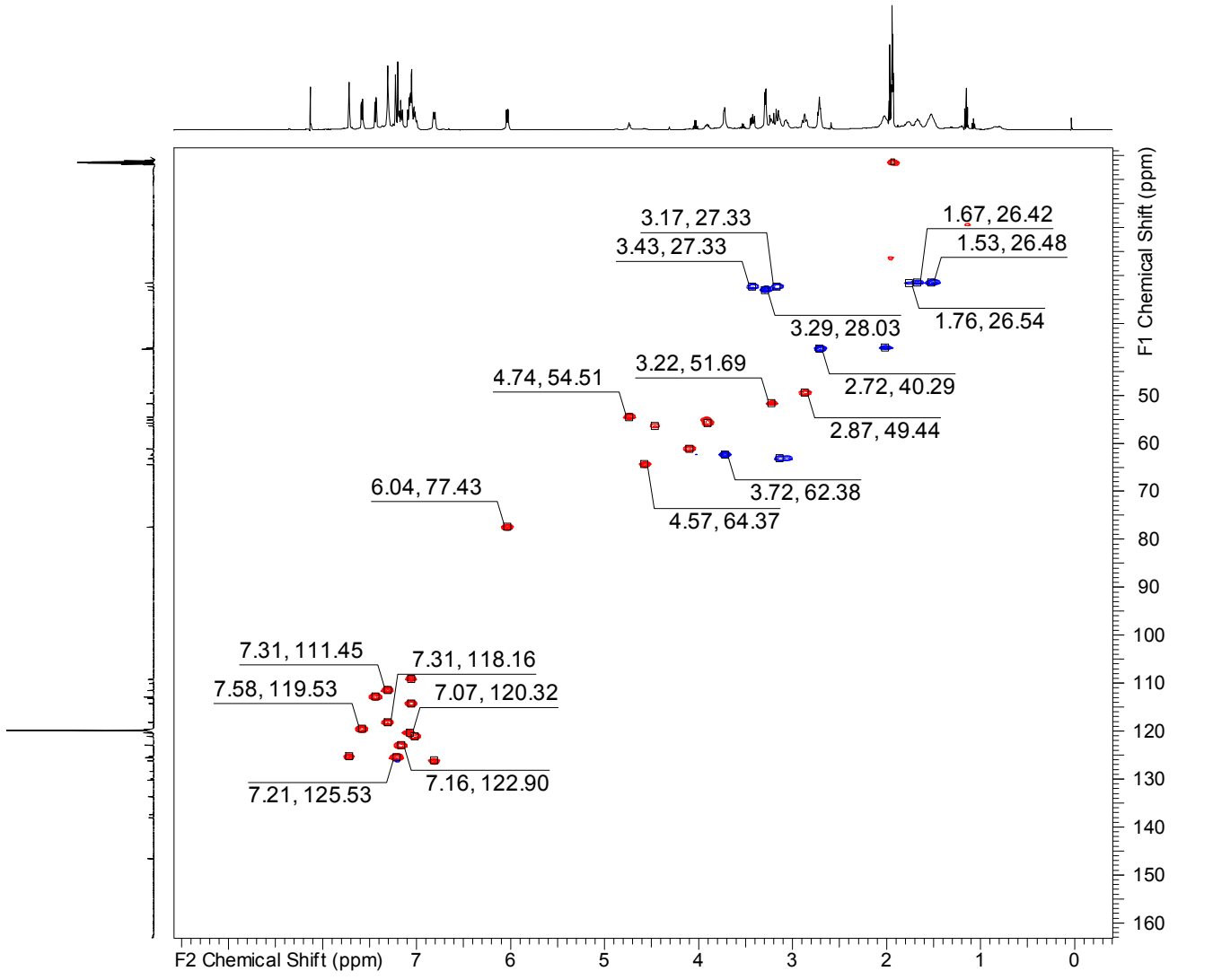

Suppl. Figure 46. HSQC spectrum of darobactin 9 in a 2:1 mixture of H_2O-d_2 acetonitrile-d_3-containing 2 % formic acid-d_2 at 45 °C and 500/125 MHz.

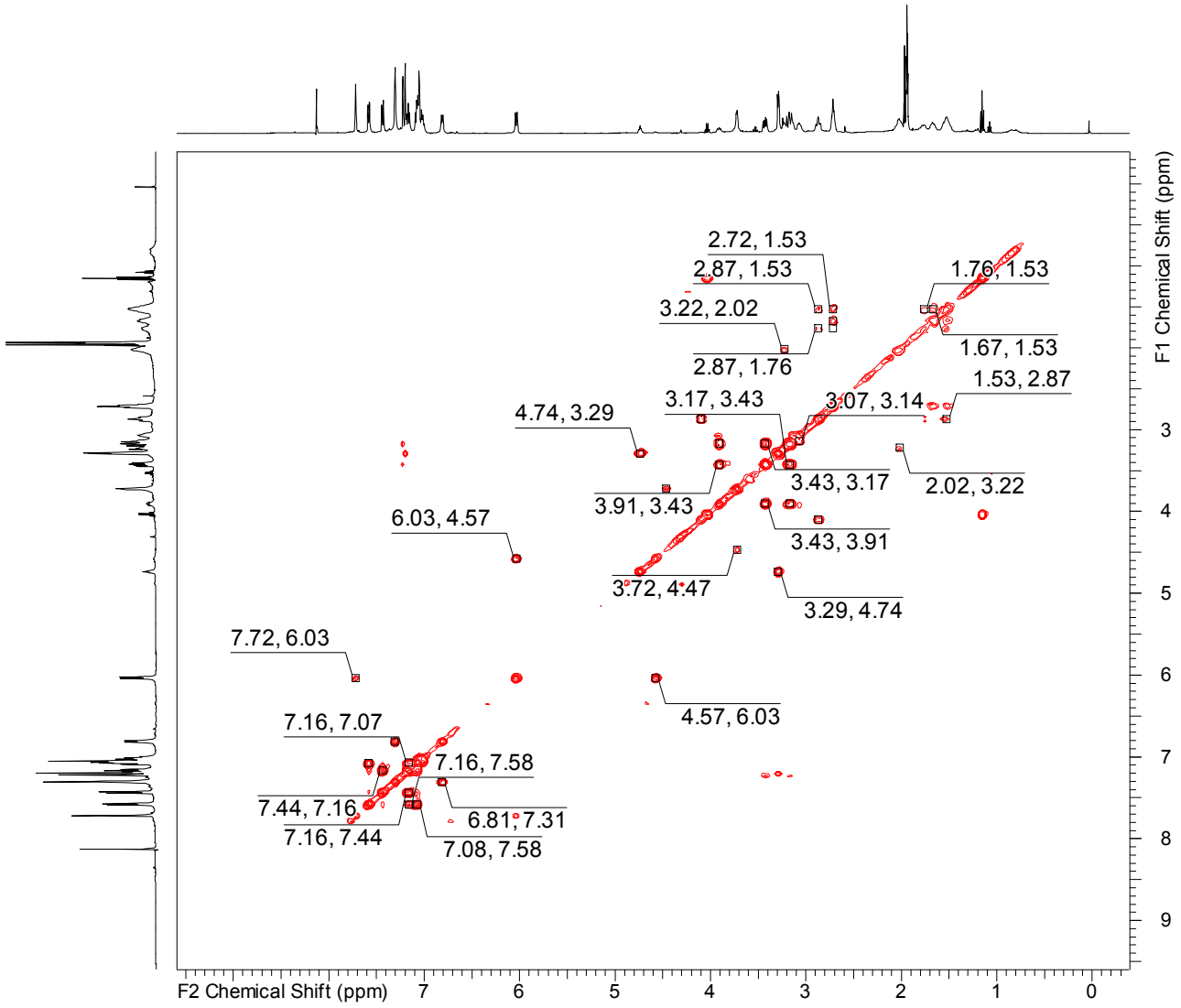

Suppl. Figure 47. COSY spectrum of darobactin 9 in a 2:1 mixture of H_2O-d_2 acetonitrile-d_3-containing 2 % formic acid-d_2 at 45 °C and 500 MHz.

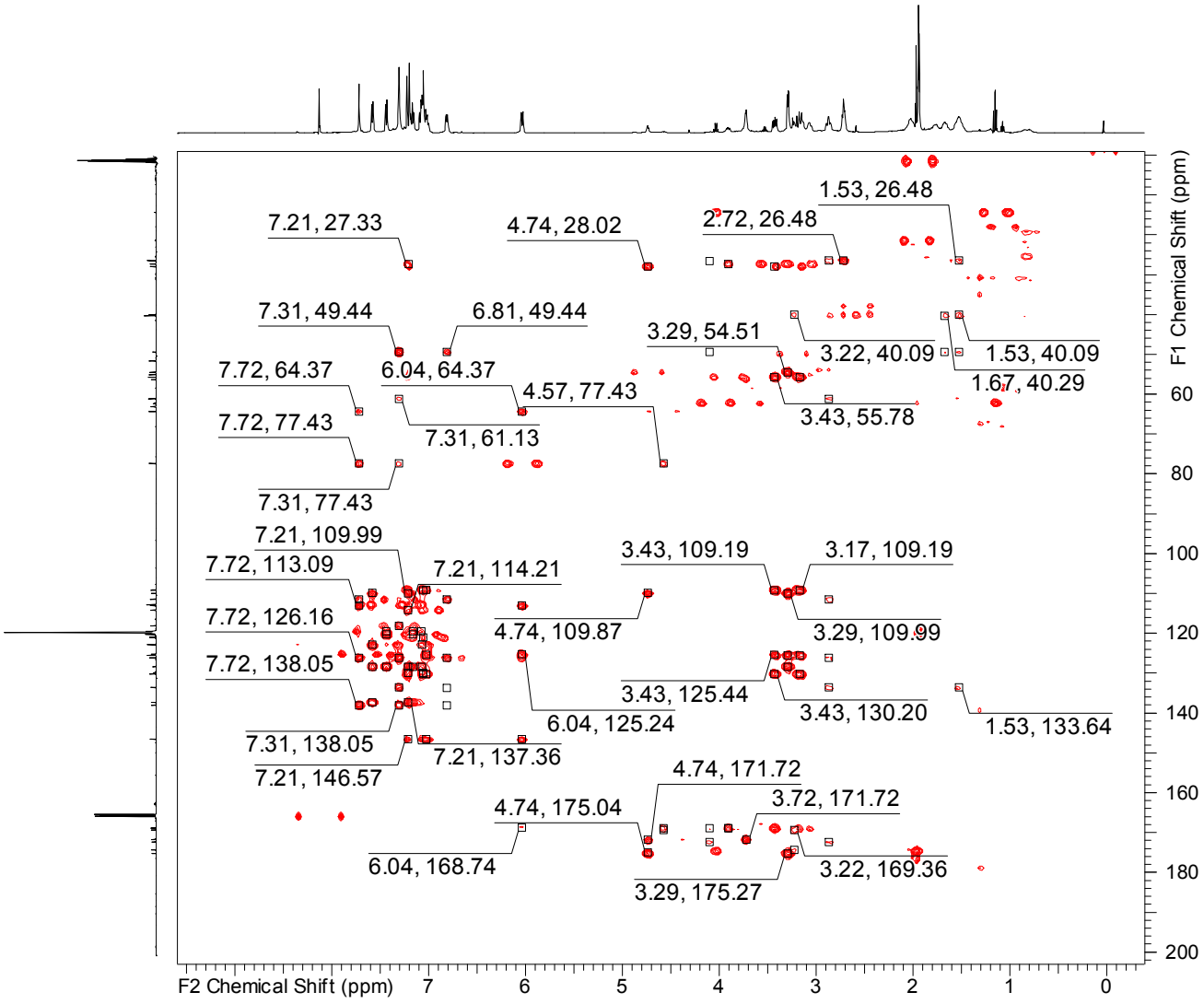

Suppl. Figure 48. HMBC spectrum of darobactin 9 in a 2:1 mixture of H_2O-d_2 acetonitrile-d_3-containing 2 % formic acid-d_2 at 45 °C and 500/125 MHz.

Suppl. Table 10. NMR chemical shifts and correlations of darobactin 9 in a 2:1 mixture of H_2O-d_2 acetonitrile-d_3-containing 2 % formic acid-d_2 at 45 °C and 500/125 MHz.

#	δ ^{13}C [ppm]	δ ^{1}H [ppm], mult (*J* [Hz])	COSY	HMBC
1	175.3	-	-	-
2	54.5	4.74, bt (5.6)	3	3, 4, 12
3	28.0	3.29, bd (5.8)	2	1, 2, 4, 5, 6
4	110.0	-	-	-
5	125.5	7.21, s	-	2, 3, 4, 6, 7, 8, 11
6	128.4	-	-	-
7	119.5	7.58, d (7.9)	8, 9	4, 6, 9, 11
8	120.3	7.07, m	7, 9	6, 9, 10
9	122.9	7.16, t (7.6)	8, 10	6, 7, 8, 11
10	112.8	7.44, d (8.2)	9	6, 7, 8
11	137.4	-	-	-
12	171.7	-	-	-
13	56.4	4.47, bs	14	-
14	62.4	3.72, bd (4.6)	13	12, 13
15	172.4	-	-	-
16	61.1	4.10, bd (9.8)	17	15, 17, 18, 19, 21
17	49.4	2.87, bt (9.8)	18, 19	16, 18, 19, 31, 32, 33
18	26.5	1.53/1.67, m	17, 19, 20	17, 19, 20, 33
19	26.5	1.76, m	17, 18, 20	16, 17, 33
20	40.3	2.72, bt (6.8)	18, 19	17
21	169.0	-	-	-
22	55.1	3.91, m	23	24
23	63.2	3.14/3.07, m	22	21
24	168.7	-	-	-
25	64.4	4.57, bd (8.5)	26	26, 27, 28, 46
26	77.4	6.04, bd (8.9)	25, 28	24, 25, 27, 28, 44
27	113.1	-	-	-
28	125.2	7.72, s	26	25, 26, 27, 29, 30, 31
29	126.2	-	-	-
30	138.0	-	-	-
31	111.5	7.31, m	32	17, 26, 28, 32, 33, 34
32	126.1	6.81, bd (7.9)	31	17, 29, 30, 31, 34
33	133.6	-	-	-
34	118.2	7.31, m	-	17, 29, 30, 31, 32, 33
35	168.9	-	-	-
36	55.8	3.91, m	37	37
37	27.3	3.43/3.17, dd (13.5, 7.1)/m	36	35, 36, 38, 40, 41, 45
38	109.2	-	-	-
39	114.2	7.06, m	-	38, 40, 45
40	129.9	-	-	-
41	125.4	7.21, d (12.2)	42	37, 38, 39, 40, 43, 44, 45
42	121.1	7.02, m	41, 43	40, 41, 43, 44, 45
43	109.1	7.06, m	42	41, 42, 44, 45
44	146.6	-	-	-
45	130.2	-	-	-
46	169.4	-	-	-
47	51.7	3.22, m	48	35, 46, 48, 49
48	40.1	2.02, m	47	46, 47, 49
49	174.4	-	-	-

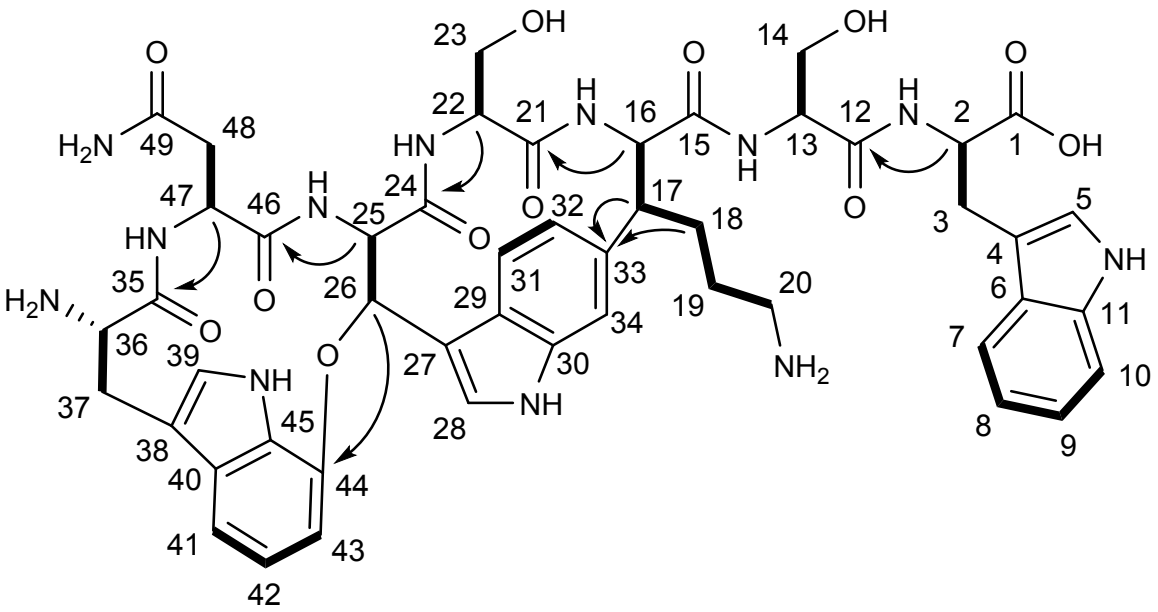

Suppl. Figure 49. Most relevant COSY (bold) and HMBC correlations (arrows) used for structure elucidation of darobactin 9 including atom numbers referred in table 8.

Protein overexpression and purification of DarF

For heterologous overexpression and purification of DarF, 6 x 1 L LB medium were inoculated with 10 mL *E. coli* BL21 (DE3) pHisSUMOTEV-darF LB seed culture each. The fermentation was performed in 5 L baffled shake flasks at 30 °C and 180 rpm (Orbitron/Multitron, Infors HT) until an OD_{600} 0.5 – 0.7 was reached. The cultures were subsequently cooled for 10 min on ice, followed by addition of 0.4 mM IPTG to induce the *T7lac* promoter regulated *darF* gene expression. Next, the cultures were grown for 18 h at 16 °C and 180 rpm.

The cells were harvested by centrifugation on an Avanti J-26 XP centrifuge (Beckman Coulter) with the JLA 8.1 rotor at 6,000 x g for 15 min at 4 °C. All the following steps were performed on ice or at 4 °C. The cell pellets were combined and re-suspended in 100 mL lysis buffer (20 mM Bis-Tris, 200 mM NaCl, 20 mM imidazole, 1 mM TCEP, pH 6.8) and two capsule of protease inhibitor (cComplete, EDTA-free from Roche, Basel, Switzerland) were added. Cells lysis was performed by passing the cell suspension two times through a cell disrupter (Constant Systems; Daventry, UK) at 30,000 psi and spun down for 25 min on an Avanti J-26 XP centrifuge with the JA 25.50 rotor at 40,000 x g and 4 °C. The supernatant was filtered using a cellulose nitrate membrane filter (5 µm pore size) and loaded onto a pre-equilibrated (lysis buffer) 5 mL HisTrap HP column (GE Healthcare, Chicago, Illinois (US)) for affinity purification. All following purification steps were performed on an Aekta go FPLC device (GE Healthcare). The HisTrap column waswashed with lysis buffer (30 column volumes) at 5 mL/min flow rate. The elution of DarF was performed using elution buffer (20 mM Bis-Tris, 200 mM NaCl, 250 mM

imidazole, 1mM TCEP, pH 6.8). The DarF-containing fractions were collected, loaded onto a pre-equilibrated (lysis buffer) Hi Prep Desalt 16/10 column (GE Healthcare) and the imidazole was removed by washing with lysis buffer (1.2 column volumes) at 10 mL/min. Subsequently, Tobacco etch virus (TEV) protease was added to the DarF-containing eluate with a ratio of 1:10 (v/v) and incubated at 4 °C for 12 h to remove the HisSUMO tag. After a second HisTrap column purification step using the same conditions as described above, the DarF-containing flow through was collected and loaded onto a pre-equilibrated (elution buffer with 10 % glycerol (w/v)) HiLoad 16/600 Superdex 200 pg gel filtration column (GE Healthcare). Size exclusion protein fractionation was performed with elution buffer plus 10 % glycerol (w/v) at 1 mL/min flow rate (1.2 column volumes). The purity of DarF was verified via SDS PAGE.

In vitro investigation of the enzyme activity of DarF

Since HHpred analysis of DarF revealed homology to zinc-dependent metalloproteases (see Supplementary Data), we tested zinc as co-factor in the *in vitro* activity assay. To remove divalent cations, which were potentially bound to DarF during the purification process, we first performed a dialysis step. The DarF eluate obtained after size exclusion chromatography had a volume of approximately 10 mL (1 mg/mL DarF) and was incubated on ice for 2 h after addition of EDTA (2 mM final concentration). After increasing the EDTA concentration (3 mM), the sample was transferred into a Slide-A Lyzer Dialysis Cassette G2, 10 MWCO (Thermo Scientific) and dialysed in 4 L elution buffer (20 mM Bis-Tris pH 6.8, 200 mM NaCl, 10 % Glycerol (w/v), 1 mM DTT) at 4 °C for 12 h under constant stirring (150 rpm, MR Hei-Standard magnetic stirrer, Heidolph Instruments, Schwabach, Germany). This dialysis step was repeated under the same conditions for another 6 h in fresh buffer.

The activity of DarF was investigated in 50 µl scale reactions (15 µM DarF, 25 µM darobactin A or 9 and 200 µM zinc in elution buffer) for 12 h at room temperature. Reactions without DarF served as controls. Each reaction was performed three times. The reactions were stopped by the addition of 150 µL acetonitrile and the samples were centrifuged at 11,000 x g for 10 min at room temperature in a table top centrifuge prior to uHPLC-MS analysis on an amaZon speed 3D ion trap MS system (Bruker Daltonics) with an Apollo II ESI source. The LC system, column and settings as well as the ESI source settings were identical as described above. Suppl. Figure 50 and Suppl. Figure 51 show representative EICs and the degradation of darobactins A and 9, respectively.

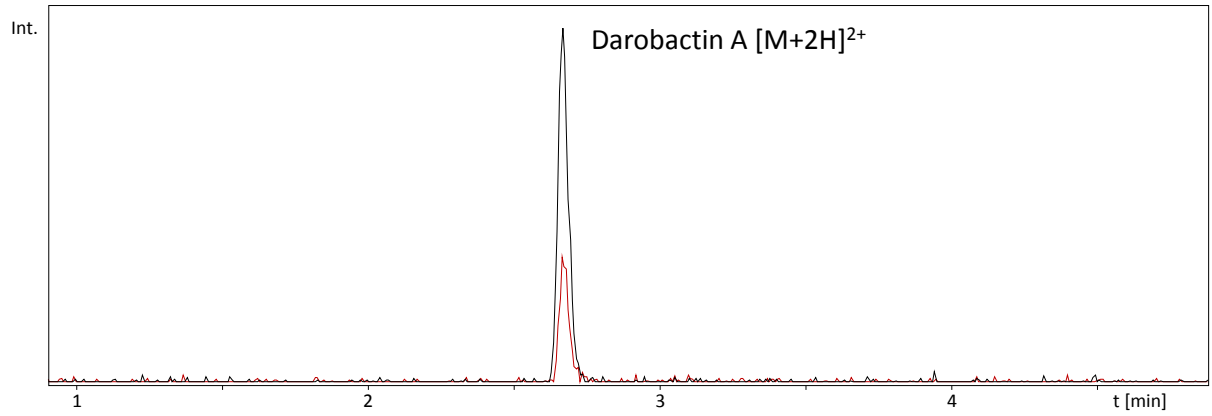

Suppl. Figure 50. Chromatogram of the in vitro *darobactin A degradation reaction by DarF (red trace) and the darobactin A control without DarF (black trace). Both traces display the darobactin A EIC for the $[M+2H]^{2+}$ species at m/z 483.71 ±0.1 Da.*

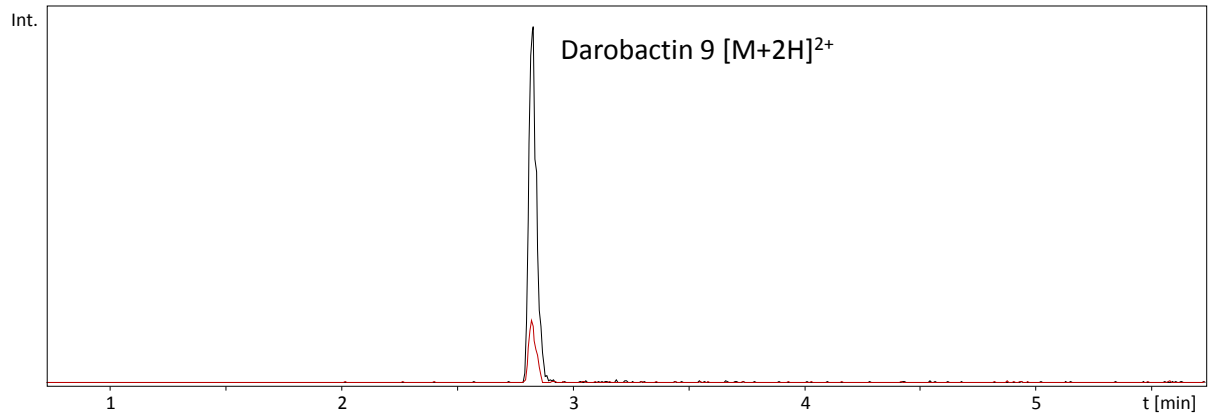

Suppl. Figure 51. Chromatogram of the in vitro *darobactin 9 degradation reaction by DarF (red trace) and the darobactin A control without DarF (black trace). Both traces display the darobactin 9 EIC for the $[M+2H]^{2+}$ species at m/z 503.21 ±0.1 Da.*

Software

Geneious version 10.1.3 (Biomatters Ltd.; Auckland, New Zealand) was used to design the modified darobactin BGC and the cloning and expression vector pNOSO *in silico*. *Chromeleon* version 6.80 (Thermo Fisher Scientific; Waltham, Massachusetts (US)) was used for LC control. *Compass HyStar* 3.2 Build 49.9 (Bruker Daltonics) was used for MS scan control. *Compass otof Control* version 3.4 (Bruker Daltonics) and *trap Control* version 8.0 (Bruker Daltonics) were used for data acquisition of the maXis 4G ToF and the amaZon speed 3D ion trap mass spectrometers, respectively. We used *Compass DataAnalysis* version 4.4 (Bruker Daltonics) to interpret MS data and *MS Excel* 2016 for the calculation of the absolute and relative production titers of darobactin A. *Topspin* 3.6.1 (Bruker Biospin) was used for NMR data acquisition and *Spectrus processor* 2019.2.1 (ACD Labs) for processing and assignment. *MS PowerPoint* 2016 was used for image processing and *ChemDraw Professional* version 17.1.0.105 (19) was used to create images of chemical structures.

Supplementary notes & References

1 J. W. Dubendorff and F. W. Studier, *J. Mol. Biol.*, 1991, **219**, 45.
2 D. Pogorevc, F. Panter, C. Schillinger, R. Jansen, S. C. Wenzel and R. Müller, *Metab. Eng.*, 2019, **55**, 201.
3 E. Beck, G. Ludwig, E. A. Auerswald, B. Reiss and H. Schaller, *Gene*, 1982, **19**, 327.
4 R. E. Rose, *Nucleic Acids Res.*, 1988, **16**, 356.
5 V. Magrini, M. L. Storms and P. Youderian, *J. Bacteriol.*, 1999, **181**, 4062.
6 J. Sambrook and D. W. Russell, *Molecular cloning: A laboratory manual*, Cold Spring Harbor Laboratory Press, Cold Spring Harbor, NY, 2001.
7 H. Liu and J. H. Naismith, *Protein Expr. Purif.*, 2009, **63**, 102.
8 Y. Zhang, F. Buchholz, J. P. Muyrers and A. F. Stewart, *Nat. Genet.*, 1998, **20**, 123.
9 S. Groß, B. Schnell, P. A. Haack, D. Auerbach and R. Müller, *Nat. Commun.*, 2021, **12**, 1696.
10 M. Wang, J. J. Carver, V. V. Phelan, L. M. Sanchez, N. Garg, Y. Peng, D. D. Nguyen, J. Watrous, C. A. Kapono, T. Luzzatto-Knaan, C. Porto, A. Bouslimani, A. V. Melnik, M. J. Meehan, W.-T. Liu, M. Crusemann, P. D. Boudreau, E. Esquenazi, M. Sandoval-Calderon, R. D. Kersten, L. A. Pace, R. A. Quinn, K. R. Duncan, C.-C. Hsu, D. J. Floros, R. G. Gavilan, K. Kleigrewe, T. Northen, R. J. Dutton, D. Parrot, E. E. Carlson, B. Aigle, C. F. Michelsen, L. Jelsbak, C. Sohlenkamp, P. Pevzner, A. Edlund, J. McLean, J. Piel, B. T. Murphy, L. Gerwick, C.-C. Liaw, Y.-L. Yang, H.-U. Humpf, M. Maansson, R. A. Keyzers, A. C. Sims, A. R. Johnson, A. M. Sidebottom, B. E. Sedio, A. Klitgaard, C. B. Larson, C. A. Boya P, D. Torres-Mendoza, D. J. Gonzalez, D. B. Silva, L. M. Marques, D. P. Demarque, E. Pociute, E. C. O'Neill, E. Briand, E. J. N. Helfrich, E. A. Granatosky, E. Glukhov, F. Ryffel, H. Houson, H. Mohimani, J. J. Kharbush, Y. Zeng, J. A. Vorholt, K. L. Kurita, P. Charusanti, K. L. McPhail, K. F. Nielsen, L. Vuong, M. Elfeki, M. F. Traxler, N. Engene, N. Koyama, O. B. Vining, R. Baric, R. R. Silva, S. J. Mascuch, S. Tomasi, S. Jenkins, V. Macherla, T. Hoffman, V. Agarwal, P. G. Williams, J. Dai, R. Neupane, J. Gurr, A. M. C. Rodriguez, A. Lamsa, C. Zhang, K. Dorrestein, B. M. Duggan, J. Almaliti, P.-M. Allard, P. Phapale, L.-F. Nothias, T. Alexandrov, M. Litaudon, J.-L. Wolfender, J. E. Kyle, T. O. Metz, T. Peryea, D.-T. Nguyen, D. VanLeer, P. Shinn, A. Jadhav, R. Muller, K. M. Waters, W. Shi, X. Liu, L. Zhang, R. Knight, P. R. Jensen, B. O. Palsson, K. Pogliano, R. G. Linington, M. Gutierrez, N. P. Lopes, W. H. Gerwick, B. S. Moore, P. C. Dorrestein and N. Bandeira, *Nat. Biotechnol.*, 2016, **34**, 828.
11 a) npatlas - The Natural Products Atlas, https://www.npatlas.org; b) J. A. van Santen, G. Jacob, A. L. Singh, V. Aniebok, M. J. Balunas, D. Bunsko, F. C. Neto, L. Castaño-Espriu, C. Chang, T. N. Clark, J. L. Cleary Little, D. A. Delgadillo, P. C. Dorrestein, K. R. Duncan, J. M. Egan, M. M. Galey, F. J. Haeckl, A. Hua, A. H. Hughes, D. Iskakova, A. Khadilkar, J.-H. Lee, S. Lee, N. LeGrow, D. Y. Liu, J. M. Macho, C. S. McCaughey, M. H. Medema, R. P. Neupane, T. J. O'Donnell, J. S. Paula, L. M. Sanchez, A. F. Shaikh, S. Soldatou, B. R. Terlouw, T. A. Tran, M. Valentine, J. J. J. van der Hooft, D. A. Vo, M. Wang, D. Wilson, K. E. Zink and R. G. Linington, *ACS Cent. Sci.*, 2019;
12 T. Baba, T. Ara, M. Hasegawa, Y. Takai, Y. Okumura, M. Baba, K. A. Datsenko, M. Tomita, B. L. Wanner and H. Mori, *Mol. Syst. Biol.*, 2006, **2**, 2006.
13 I. Wiegand, K. Hilpert and R. E. W. Hancock, *Nat. Protoc.*, 2008, **3**, 163.
14 A. Sikandar, K. Cirnski, G. Testolin, C. Volz, M. Brönstrup, O. V. Kalinina, R. Müller and J. Koehnke, *J. Am. Chem. Soc.*, 2018, **140**, 16641.